



The crust of Cathaysia: Age, assembly and reworking of two terranes

Xisheng Xu^{a,b,*}, Suzanne Y. O'Reilly^b, W.L. Griffin^b,
Xiaolei Wang^{a,b}, N.J. Pearson^b, Zhenyu He^a

^a State Key Laboratory for Mineral Deposits Research, Department of Earth Sciences, Nanjing University, Nanjing 210093, China

^b GEMOC ARC National Key Centre, Macquarie University, NSW 2109, Australia

Received 10 December 2006; received in revised form 19 April 2007; accepted 24 April 2007

Abstract

U–Pb dating and Hf-isotope data from detrital zircons have been used to analyse the crustal evolution of the eastern and western parts of the Cathaysia Block in SE China. Zircons from the Oujiang River in eastern Cathaysia indicate that the basement is dominantly Paleoproterozoic (1850–1870 Ma, 2100–2400 Ma) in age with minor Archean components; it was extensively reworked in Jurassic–Cretaceous time (100–155 Ma) to produce the widespread Yanshanian magmatic suite. Both the 1850–1870 Ma event and the Yanshanian magmatism show wide ranges in Hf-isotope composition, consistent with mixing between crustal and juvenile magmas. Marked downstream changes in the relative proportions of zircon age populations emphasize the care required in using detrital zircon data to estimate continental growth rates. Zircons from the North River indicate that the crust of western Cathaysia was generated mainly during Neoproterozoic time, although it contains some Archean (2500–3500 Ma) to Mesoproterozoic components. This crust was strongly reworked during Caledonian (ca. 450 Ma), Indosian (ca. 240 Ma) and Early Yanshanian (ca. 160 Ma) thermal events; there is little evidence for juvenile crustal growth in any of these events. Although the Yanshanian granitoids of the eastern and western parts of the Cathaysia give similar mean Hf model ages (consistent with published Nd model ages), this is a coincidence; they have different crustal sources. The distinct patterns of crustal evolution suggest that eastern and western Cathaysia may represent separate microcontinents, accreted to the older Yangtze craton and transposed by extensive strike-slip faults.

© 2007 Elsevier B.V. All rights reserved.

Keywords: Zircon geochronology; Zircon Hf isotopes; Crustal evolution; Crust–mantle interaction; Cathaysia tectonism; SE China crust

1. Introduction

Understanding the evolution of individual domains of Precambrian crust is essential to geodynamic reconstructions, and to models for the distribution of economic mineralisation (e.g., Barth et al., 2000; Claesson et al.,

2001; Z.X. Li et al., 2003a; Lan et al., 2001, 2003; Neves, 2003). The combination of U–Pb dating and Hf-isotope analysis of detrital zircons from modern drainages provides a relatively rapid way to unravel the crustal evolution of terrane-scale continental blocks (e.g., Cawood et al., 2003; Griffin et al., 2004, 2006; Rino et al., 2004; Iizuka et al., 2005; Condie et al., 2005). The South China region has a complex tectonic history, and consists of two major Precambrian continental blocks: the Yangtze Block to the northwest, and the Cathaysia Block to the southeast, defined by a series of major faults (Fig. 1). The basement exposures of the

* Corresponding author at: State Key Laboratory for Mineral Deposits Research, Department of Earth Sciences, Nanjing University, Nanjing 210093, China. Fax: +86 25 83686016.

E-mail address: xsxu@nju.edu.cn (X. Xu).

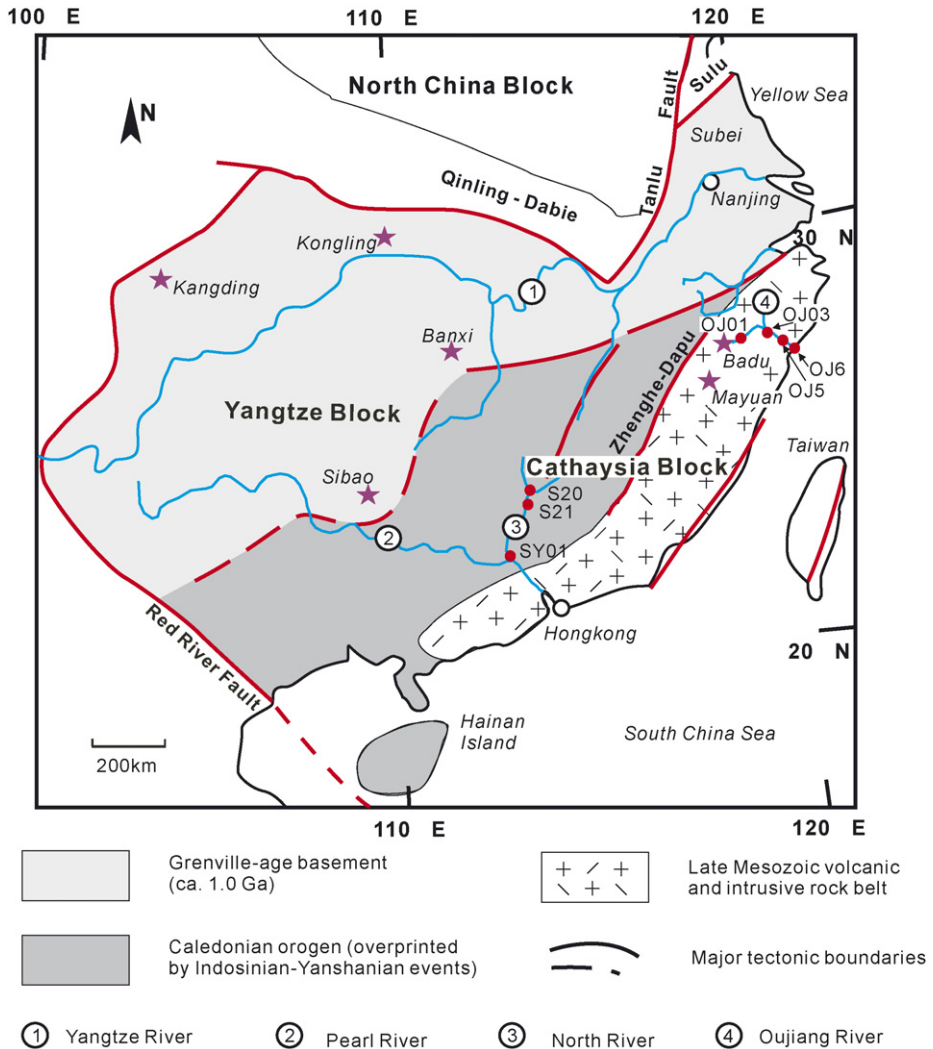


Fig. 1. River systems and sample locations in Cathaysia region.

Yangtze Block include several groups of Proterozoic to Archean rocks, i.e., Kongling, Kangding, Sibao, and Banxi (Fig. 1) (Ames et al., 1996; Gao et al., 1999; Zhao and Peter, 1999 and references therein; Qiu et al., 2000; Li et al., 2002). Recent studies of crustal zircons in deep-seated intrusive rocks (Zheng et al., 2006) indicate that the basement to the Yangtze Block contains a higher proportion of Archean rocks than is indicated by these outcropping units.

The concept of the Cathaysia Block, named after the “Cathaysia old continent” of Grabau (1924), is based on the observation that the basement is unconformably overlain by Devonian sediments. This concept has gained wide acceptance in the past few years, largely due to isotopic and geochronological work (e.g., Shui et al., 1987; Jahn et al., 1990; Chen and Jahn, 1998; Li et al.,

1998, 2000; Li, 1998). On the other hand, there has been a long controversy regarding the age and distribution of the basement rocks, which are poorly exposed (e.g., Hu et al., 1991a,b; Gan et al., 1993; Chen and Jahn, 1998; Zhao and Peter, 1999; Hong et al., 1999). Although a large database of Nd model ages (e.g., Chen and Jahn, 1998; Shen et al., 2007), mainly on Late Mesozoic magmatic rocks, shows that the Cathaysia Block may have widespread Proterozoic basement, the ubiquitous Proterozoic model ages may have alternative interpretations. The database also shows that Nd model ages tend to be older in the interior parts of Cathaysia (western Cathaysia) and younger in the coastal areas (eastern Cathaysia). The boundary between east and west Cathaysia is roughly along Zhenghe-Dapu fault as defined by Chen and Jahn (1998).

In the coastal regions of southeast China (eastern Cathaysia), Late Mesozoic magmatism is well developed. Field relations, Sr–Nd isotopes of whole-rocks (Chen and Jahn, 1998) and Hf-isotope data on zircons (e.g., Griffin et al., 2002) suggest that this magmatism includes both juvenile mantle-derived components, and magmas derived from the remelting of older crust; in some cases mixing between these components can be clearly documented. In the interior parts of southeastern China (western Cathaysia), a Paleozoic orogen has been overprinted by Mesozoic events, and the nature of the underlying basement rocks is still not clear.

The combined *in situ* U–Pb and Hf-isotope analysis of single grain detrital zircons is a powerful tool for the analysis of crustal evolution (e.g., Griffin et al., 2004, 2006). While conventional provenance studies using U–Pb analysis of detrital zircons produce only age spectra, the Hf-isotope analyses add a layer of information on the sources (juvenile mantle versus reworked crust) of the host magma for each zircon grain. This information makes it possible to examine the nature of major magmatic events, rather than simply their timing. This approach can be applied on scales ranging from the continental (e.g., Iizuka et al., 2005) to single drainages. In this study, we have worked at an intermediate scale, sampling drainages of 15,000–50,000 km², to examine possible terrane-scale differences in crustal evolution across a major tectonic block.

The age of the Cathaysia crustal basement and its evolution has been discussed based on wide Sr–Nd data (e.g., Gilder et al., 1996; Chen and Jahn, 1998; Shen et al., 2007). Incorporating these wide coverage Sr–Nd isotope data, LAM-ICPMS U–Pb dating and Hf-isotope analysis of zircons separated from sand samples from the Oujiang River (eastern Cathaysia) and the North River (western Cathaysia) have been carried out to further constrain the age of the basement and its evolution in these two areas. The data suggest that eastern and western Cathaysia have followed distinctly different crustal evolution paths; we discuss the tectonic and geodynamic consequences of this observation.

2. River catchments and sample preparation

The Oujiang River (Fig. 1) is the second largest river system in Zhejiang Province of eastern China, with a catchment area of 18,000 km²; the main river is 388 km long with a drop of 600 m. It crosses the eastern part of the Cathaysia block, starting from the basement exposure of the Badu group (ca. 1800 Ma; Gan et al., 1995, 1996), and flows across a terrain that is increasingly dominated by Yanshanian magmatic rocks (140–100 Ma) toward

the coast. The North River is a branch of the Pearl River, with a catchment area of 46,710 km². The main river is 468 km long and the river system lies entirely within the western part of the Cathaysia Block.

Sand samples have been systematically collected from the upper to the lower reaches of each river, with sampling concentrated at the intersections of major tributaries. About 10 kg of sand were collected in each locality. Hundreds of zircons were separated from each sample through panning, followed by heavy-liquid separation and handpicking.

Sixty to hundred zircons from each sand sample were selected under a Nikon binocular microscope to cover different morphological populations (including variations in elongation, colour and crystal face development), and the selected zircons were mounted in epoxy blocks and polished for analysis.

Data on Si, Zr and Hf contents, and combined backscattered electron/cathodoluminescence (BSE/CL) images of the selected zircons, were collected using a Camebax SX100 electron microprobe (EMP) at the GEMOC Key Centre in Macquarie University, Australia. Forty to sixty zircons from each sample were selected for U–Pb dating and Hf-isotope analysis by examination of the internal structure and composition of each grain.

3. Methods for isotope analysis

3.1. U–Pb dating

The data reported here (Table 1) were obtained using an Agilent 7500 ICPMS, coupled to a New Wave Research 213 nm microprobe at GEMOC, Macquarie University, Australia. A description of the procedure is given by Jackson et al. (2004). The repetition rate used for all analyses was 5 Hz, the aperture beam diameter/iris setting is 15%, beam expander is 0 and the incident pulse energy is about 0.08–0.1 mJ. The spot size for most of the 213 nm laser analyses is about 40–50 μm.

Mass discrimination of the mass spectrometer and residual elemental fractionation were corrected by calibration against a homogeneous standard zircon, GEMOC/GJ-1 (609 Ma). Samples are analysed in “runs” of ca. 20 analyses, which include 12 unknowns, bracketed, beginning and end, by two to four analyses of the standard. The “unknowns” include two near-concordant standard zircons, 91500 (Wiedenbeck et al., 1995) and Mud Tank (Black and Gulson, 1978), which are analysed in every run as an independent control on reproducibility and instrument stability. The precision and accuracy obtained on those standards, and several others, by LAM-ICPMS are discussed in detail by Jackson et al. (2004).

OJ1-62	95	186	0.51	0.11024	0.00234	4.576	0.084	0.3010	0.0032	0.0870	0.0009	1803	39	1745	15	1696	16	1687	16
OJ1-63	65	268	0.24	0.11034	0.00190	3.726	0.051	0.2449	0.0026	0.0708	0.0008	1805	32	1577	11	1412	13	1383	14
OJ1-64	130	575	0.23	0.11175	0.00225	2.988	0.050	0.1939	0.0021	0.0560	0.0008	1828	37	1404	13	1142	11	1101	15
OJ1-65	38	293	0.13	0.11222	0.00121	4.445	0.049	0.2873	0.0030	0.0857	0.0013	1836	9	1721	9	1628	15	1661	25
OJ1-66	22	743	0.03	0.11298	0.00134	4.040	0.050	0.2594	0.0029	0.0782	0.0018	1848	10	1642	10	1487	15	1521	33
OJ1-67	12	503	0.02	0.11233	0.00185	3.853	0.048	0.2488	0.0027	0.0718	0.0008	1837	30	1604	10	1432	14	1401	15
OJ1-69	154	151	1.03	0.04911	0.00097	0.159	0.003	0.0235	0.0003	0.0074	0.0001	153	25	150	3	150	2	149	3
OJ1-75	35	107	0.32	0.15162	0.00205	7.740	0.099	0.3703	0.0038	0.1050	0.0027	2364	10	2201	12	2031	18	2019	49
OJ1-76	116	166	0.70	0.11287	0.00136	4.800	0.058	0.3084	0.0033	0.0894	0.0018	1846	10	1785	10	1733	16	1730	33
OJ1-77	14	411	0.04	0.11260	0.00165	3.554	0.038	0.2289	0.0023	0.0660	0.0007	1842	27	1539	8	1329	12	1293	13
OJ1-78	261	186	1.40	0.04932	0.00175	0.163	0.006	0.0240	0.0004	0.0077	0.0002	163	53	153	5	153	2	155	5
OJ1-79	70	192	0.36	0.13091	0.00240	5.922	0.089	0.3281	0.0034	0.0932	0.0010	2110	33	1964	13	1829	17	1802	18
OJ1-83	23	336	0.07	0.11325	0.00149	4.365	0.060	0.2796	0.0032	0.0835	0.0023	1852	11	1706	11	1589	16	1621	43
OJ1-84	66	189	0.35	0.15042	0.00257	8.398	0.113	0.4049	0.0043	0.1135	0.0012	2351	30	2275	12	2192	20	2173	22
OJ1-85	39	472	0.08	0.11265	0.00206	3.333	0.048	0.2146	0.0024	0.0619	0.0007	1843	34	1489	11	1253	13	1214	13
OJ1-87	4	1059	0.00	0.05209	0.00119	0.260	0.005	0.0361	0.0005	0.0114	0.0007	289	54	234	4	229	3	228	13
OJ1-88	253	253	1.00	0.05499	0.00545	0.172	0.017	0.0227	0.0004	0.0071	0.0001	412	227	161	15	144	2	142	2
OJ1-89	3	108	0.03	0.05589	0.00183	0.303	0.009	0.0393	0.0005	0.0122	0.0011	448	74	268	7	248	3	246	21
OJ1-90	80	403	0.20	0.11298	0.00129	4.583	0.053	0.2943	0.0031	0.0857	0.0016	1848	9	1746	10	1663	15	1661	29
OJ1-91	55	793	0.07	0.10184	0.00186	1.565	0.023	0.1115	0.0012	0.0325	0.0006	1658	35	956	9	681	7	646	12
OJ3-01	139	694	0.20	0.09325	0.00111	1.061	0.012	0.0825	0.0008	0.0190	0.0004	1493	10	734	6	511	5	380	7
OJ3-02	3795	594	6.39	0.04809	0.00114	0.112	0.003	0.0169	0.0002	0.0051	0.0001	104	32	108	2	108	1	103	3
OJ3-04	204	263	0.78	0.04848	0.00100	0.136	0.003	0.0204	0.0002	0.0066	0.0001	123	26	130	2	130	2	133	3
OJ3-06	17	1098	0.02	0.11261	0.00178	3.718	0.043	0.2395	0.0026	0.0691	0.0008	1842	29	1575	9	1384	13	1350	15
OJ3-09	68	120	0.57	0.08373	0.00246	1.775	0.048	0.1538	0.0017	0.0458	0.0005	1286	59	1036	18	922	10	904	10
OJ3-10	110	219	0.50	0.10702	0.00296	3.652	0.093	0.2475	0.0027	0.0718	0.0007	1749	52	1561	20	1425	14	1401	14
OJ3-11	77	128	0.60	0.12493	0.00373	5.424	0.149	0.3149	0.0037	0.0899	0.0011	2028	54	1889	24	1765	18	1740	19
OJ3-12	21	195	0.11	0.06631	0.00213	0.801	0.024	0.0876	0.0011	0.0268	0.0007	816	69	597	13	541	6	534	13
OJ3-13	396	406	0.97	0.04867	0.00112	0.134	0.003	0.0199	0.0003	0.0064	0.0002	132	30	127	3	127	2	129	4
OJ3-14	248	220	1.13	0.04864	0.00181	0.138	0.005	0.0205	0.0003	0.0065	0.0003	131	57	131	4	131	2	130	6
OJ3-15	1283	964	1.33	0.04872	0.00090	0.141	0.003	0.0210	0.0002	0.0067	0.0002	134	22	134	2	134	2	134	4
OJ3-17	111	202	0.55	0.11329	0.00124	4.964	0.056	0.3178	0.0034	0.0946	0.0014	1853	9	1813	9	1779	16	1827	26
OJ3-18	96	471	0.20	0.11319	0.00119	4.636	0.050	0.2971	0.0031	0.0876	0.0012	1851	9	1756	9	1677	15	1697	22
OJ3-19	258	1331	0.19	0.11145	0.00191	2.218	0.030	0.1443	0.0015	0.0417	0.0004	1823	32	1187	10	869	8	825	8
OJ3-22	77	92	0.83	0.05018	0.00202	0.147	0.006	0.0212	0.0003	0.0068	0.0002	203	64	139	5	135	2	138	5
OJ3-23	228	334	0.68	0.04983	0.00087	0.158	0.003	0.0231	0.0003	0.0074	0.0002	187	20	149	2	147	2	150	3
OJ3-24	480	382	1.26	0.05013	0.00147	0.137	0.004	0.0198	0.0003	0.0062	0.0002	201	41	130	3	127	2	126	4
OJ3-25	48	46	1.06	0.05283	0.00610	0.171	0.019	0.0234	0.0007	0.0075	0.0006	322	195	160	17	149	5	151	11
OJ3-26	165	172	0.96	0.04849	0.00109	0.133	0.003	0.0199	0.0002	0.0063	0.0001	123	31	127	3	127	1	127	3
OJ3-27	816	501	1.63	0.04940	0.00123	0.159	0.004	0.0234	0.0003	0.0074	0.0003	167	33	150	3	149	2	149	5
OJ3-29	300	441	0.68	0.12428	0.00137	5.691	0.063	0.3321	0.0035	0.0969	0.0016	2019	9	1930	10	1849	17	1870	29
OJ3-30	456	448	1.02	0.15833	0.00206	9.426	0.122	0.4318	0.0046	0.1206	0.0031	2438	10	2380	12	2314	21	2302	56
OJ3-31	299	199	1.50	0.04804	0.00099	0.107	0.002	0.0161	0.0002	0.0051	0.0001	101	27	103	2	103	1	104	2
OJ3-32	51	368	0.14	0.11372	0.00172	4.431	0.062	0.2826	0.0028	0.0787	0.0028	1860	12	1718	12	1604	14	1531	53
OJ3-33	56	1329	0.04	0.13263	0.00188	5.593	0.061	0.3058	0.0027	0.0868	0.0008	2133	25	1915	9	1720	13	1682	15
OJ3-34	41	32	1.28	0.04860	0.00537	0.136	0.015	0.0202	0.0004	0.0066	0.0003	129	207	129	13	129	3	134	6
OJ3-35	111	247	0.45	0.11354	0.00135	4.597	0.050	0.2937	0.0027	0.0871	0.0019	1857	9	1749	9	1660	14	1687	35
OJ3-36	100	41	2.45	0.05049	0.00471	0.163	0.015	0.0235	0.0005	0.0077	0.0003	218	169	154	13	150	3	154	6
OJ3-37	257	259	0.99	0.04844	0.00151	0.134	0.004	0.0200	0.0003	0.0070	0.0002	121	47	127	4	128	2	141	5
OJ3-38	38	730	0.05	0.11128	0.00159	3.296	0.037	0.2148	0.0019	0.0620	0.0006	1820	27	1480	9	1254	10	1217	11
OJ3-39	149	288	0.52	0.10669	0.00238	3.987	0.079	0.2711	0.0028	0.0786	0.0008	1744	42	1632	16	1546	14	1530	14

OJ5-14	398	514	0.78	0.04920	0.00075	0.148	0.002	0.0219	0.0002	0.0068	0.0001	157	17	141	2	140	1	137	2
OJ5-15	166	96	1.73	0.04895	0.00216	0.149	0.006	0.0220	0.0003	0.0072	0.0002	145	74	141	6	140	2	145	4
OJ5-16	156	159	0.98	0.04872	0.00122	0.140	0.003	0.0209	0.0002	0.0069	0.0002	134	36	133	3	133	1	138	3
OJ5-17	571	722	0.79	0.13303	0.00429	5.757	0.171	0.3139	0.0039	0.0891	0.0011	2138	58	1940	26	1760	19	1724	20
OJ5-18	150	290	0.52	0.15628	0.00286	8.371	0.132	0.3885	0.0036	0.1085	0.0010	2416	32	2272	14	2116	17	2082	18
OJ5-19	550	521	1.06	0.04881	0.00102	0.132	0.003	0.0196	0.0002	0.0063	0.0002	139	27	126	2	125	1	128	3
OJ5-20	264	429	0.62	0.04899	0.00103	0.157	0.003	0.0232	0.0003	0.0073	0.0002	147	27	148	3	148	2	148	4
OJ5-21	170	220	0.77	0.04813	0.00173	0.104	0.004	0.0156	0.0002	0.0053	0.0002	106	57	100	3	100	1	106	4
OJ5-22	568	725	0.78	0.04863	0.00111	0.140	0.003	0.0209	0.0003	0.0069	0.0003	130	30	133	3	133	2	139	5
OJ5-23	227	269	0.84	0.04912	0.00158	0.161	0.005	0.0238	0.0003	0.0078	0.0003	154	48	151	4	151	2	157	6
OJ5-24	95	93	1.02	0.04886	0.00209	0.140	0.006	0.0208	0.0003	0.0069	0.0003	141	71	133	5	132	2	139	5
OJ5-26	81	95	0.85	0.04838	0.00337	0.117	0.008	0.0175	0.0003	0.0058	0.0004	118	115	112	7	112	2	117	7
OJ5-28	352	713	0.49	0.05287	0.00138	0.139	0.003	0.0191	0.0002	0.0067	0.0003	323	35	132	3	122	1	134	5
OJ5-29	148	126	1.17	0.04905	0.00224	0.144	0.006	0.0213	0.0003	0.0066	0.0003	150	75	136	6	136	2	132	5
OJ5-30	225	594	0.38	0.05073	0.00070	0.248	0.003	0.0354	0.0004	0.0114	0.0002	229	14	225	3	224	2	230	5
OJ5-31	393	492	0.80	0.04798	0.00117	0.098	0.002	0.0148	0.0002	0.0048	0.0001	98	33	95	2	95	1	97	3
OJ5-33	290	285	1.02	0.04898	0.00100	0.144	0.003	0.0214	0.0002	0.0068	0.0002	147	27	137	2	136	1	136	3
OJ5-34	219	126	1.73	0.04926	0.00207	0.161	0.007	0.0237	0.0003	0.0072	0.0003	160	68	151	6	151	2	145	5
OJ5-35	95	112	0.85	0.11301	0.00148	4.908	0.059	0.3150	0.0030	0.0921	0.0023	1848	10	1804	10	1765	15	1781	42
OJ5-37	150	95	1.58	0.04964	0.00241	0.167	0.008	0.0243	0.0004	0.0078	0.0003	178	80	156	7	155	2	156	6
OJ5-38	263	229	1.15	0.04880	0.00111	0.146	0.003	0.0216	0.0002	0.0067	0.0002	138	31	138	3	138	2	136	3
OJ5-39	40	551	0.07	0.11369	0.00214	3.426	0.064	0.2185	0.0027	0.0681	0.0035	1859	17	1510	15	1274	14	1331	66
OJ5-41	156	142	1.10	0.05057	0.00153	0.234	0.007	0.0336	0.0004	0.0103	0.0004	221	44	214	6	213	3	208	8
OJ5-42	224	149	1.50	0.04897	0.00167	0.155	0.005	0.0229	0.0003	0.0076	0.0002	146	53	146	5	146	2	152	4
OJ5-43	101	98	1.03	0.04888	0.00156	0.141	0.004	0.0209	0.0002	0.0070	0.0002	142	52	134	4	133	1	141	3
OJ5-44	155	246	0.63	0.04856	0.00172	0.141	0.005	0.0210	0.0003	0.0071	0.0003	127	54	134	4	134	2	143	6
OJ5-46	367	270	1.36	0.04858	0.00102	0.137	0.003	0.0204	0.0002	0.0066	0.0001	128	28	130	2	130	1	133	3
OJ5-47	220	444	0.49	0.04866	0.00074	0.143	0.002	0.0214	0.0002	0.0069	0.0001	131	17	136	2	136	1	139	3
OJ5-48	35	284	0.12	0.13057	0.00159	6.442	0.069	0.3578	0.0032	0.1015	0.0024	2106	9	2038	9	1972	15	1955	43
OJ5-49	452	470	0.96	0.04864	0.00081	0.140	0.002	0.0208	0.0002	0.0065	0.0001	131	19	133	2	133	1	130	3
OJ5-50	541	567	0.95	0.04906	0.00113	0.151	0.003	0.0223	0.0002	0.0068	0.0003	151	31	143	3	142	1	138	5
OJ5-51	429	1491	0.29	0.11228	0.00133	4.158	0.046	0.2686	0.0026	0.0791	0.0017	1837	9	1666	9	1534	13	1538	32
OJ5-52	296	426	0.69	0.04927	0.00078	0.176	0.003	0.0259	0.0003	0.0082	0.0002	161	18	165	2	165	2	165	4
OJ5-53	85	378	0.23	0.11268	0.00161	4.332	0.056	0.2788	0.0026	0.0853	0.0027	1843	11	1699	11	1586	13	1654	50
OJ5-55	199	208	0.96	0.04912	0.00109	0.163	0.003	0.0240	0.0002	0.0081	0.0002	154	30	153	3	153	2	162	4
OJ5-56	197	239	0.83	0.10632	0.00286	4.404	0.108	0.3004	0.0033	0.0872	0.0009	1737	50	1713	20	1694	16	1690	16
OJ5-58	325	222	1.46	0.04857	0.00123	0.134	0.003	0.0201	0.0002	0.0065	0.0002	127	37	128	3	128	1	131	3
OJ5-59	171	102	1.68	0.04879	0.00174	0.143	0.005	0.0213	0.0003	0.0068	0.0002	138	58	136	4	136	2	136	3
OJ5-60	227	229	0.99	0.04883	0.00168	0.146	0.005	0.0217	0.0003	0.0070	0.0003	140	52	138	4	138	2	141	5
OJ5-61	73	272	0.27	0.11490	0.00132	5.368	0.058	0.3389	0.0033	0.0999	0.0019	1878	9	1880	9	1881	16	1925	35
OJ5-63	485	378	1.28	0.04872	0.00241	0.142	0.007	0.0211	0.0004	0.0066	0.0004	134	77	135	6	135	2	132	9
OJ5-64	123	870	0.14	0.11335	0.00201	3.691	0.066	0.2362	0.0029	0.0631	0.0029	1854	16	1569	14	1367	15	1237	55
OJ5-66	72	196	0.37	0.11077	0.00212	4.102	0.067	0.2685	0.0027	0.0776	0.0008	1812	36	1655	13	1533	14	1511	14
OJ5-67	111	806	0.14	0.23034	0.00321	14.884	0.161	0.4687	0.0041	0.1261	0.0011	3054	23	2808	10	2478	18	2401	20
OJ5-68	444	371	1.20	0.04946	0.00202	0.146	0.006	0.0214	0.0003	0.0069	0.0004	170	63	138	5	136	2	140	8
OJ5-69	523	629	0.83	0.04898	0.00152	0.149	0.004	0.0221	0.0003	0.0073	0.0004	147	45	141	4	141	2	147	8
OJ6-01	130	175	0.74	0.05073	0.00215	0.245	0.010	0.0351	0.0004	0.0111	0.0001	229	100	223	8	222	2	222	2
OJ6-02	51	39	1.31	0.05003	0.00532	0.130	0.013	0.0189	0.0005	0.0066	0.0004	196	187	124	12	121	3	133	7
OJ6-03	245	162	1.51	0.04605	0.00224	0.131	0.006	0.0206	0.0003	0.0067	0.0002	0	105	125	5	131	2	135	3
OJ6-04	305	198	1.54	0.04862	0.00217	0.142	0.006	0.0211	0.0003	0.0066	0.0003	130	71	135	5	135	2	132	5
OJ6-05	168	112	1.50	0.04849	0.00206	0.118	0.005	0.0176	0.0002	0.0062	0.0002	123	70	113	4	112	2	125	4

OJ6-63	239	424	0.56	0.04881	0.00090	0.141	0.003	0.0209	0.0002	0.0067	0.0002	139	22	134	2	133	1	136	3
OJ6-64	75	580	0.13	0.11378	0.00128	4.528	0.048	0.2887	0.0027	0.0848	0.0016	1861	8	1736	9	1635	14	1645	29
OJ6-65	74	55	1.36	0.04808	0.00348	0.104	0.007	0.0156	0.0003	0.0051	0.0002	103	126	100	7	100	2	102	4
OJ6-66	217	124	1.75	0.04791	0.00261	0.097	0.005	0.0147	0.0002	0.0047	0.0002	95	89	94	5	94	1	94	4
OJ6-67	288	630	0.46	0.04896	0.00101	0.150	0.003	0.0223	0.0003	0.0075	0.0003	146	26	142	3	142	2	151	5
OJ6-69	207	221	0.93	0.04866	0.00126	0.136	0.003	0.0203	0.0002	0.0064	0.0002	131	36	129	3	129	2	129	4
OJ6-70	256	227	1.13	0.05036	0.00142	0.149	0.004	0.0215	0.0002	0.0064	0.0002	212	41	141	4	137	2	129	5
OJ6-71	398	353	1.13	0.04866	0.00091	0.132	0.002	0.0197	0.0002	0.0062	0.0002	131	23	126	2	126	1	124	3
OJ6-73	323	410	0.79	0.04916	0.00078	0.139	0.002	0.0206	0.0002	0.0066	0.0001	155	18	132	2	131	1	132	2
OJ6-74	163	233	0.70	0.05012	0.00102	0.143	0.003	0.0207	0.0002	0.0069	0.0002	201	26	136	2	132	1	139	3
OJ6-75	85	98	0.87	0.05012	0.00200	0.121	0.005	0.0175	0.0002	0.0054	0.0002	201	66	116	4	112	1	109	3
OJ6-76	296	207	1.43	0.05086	0.00217	0.146	0.006	0.0209	0.0003	0.0067	0.0003	234	66	139	5	133	2	135	5
OJ6-77	228	191	1.19	0.04909	0.00109	0.137	0.003	0.0203	0.0002	0.0064	0.0001	152	30	131	3	130	1	129	3
OJ6-78	205	365	0.56	0.04896	0.00134	0.133	0.004	0.0198	0.0003	0.0063	0.0002	146	39	127	3	126	2	128	5
OJ6-79	199	174	1.15	0.05054	0.00348	0.142	0.009	0.0204	0.0005	0.0074	0.0005	220	112	135	8	130	3	149	10
OJ6-80	92	224	0.41	0.11442	0.00138	4.822	0.054	0.3056	0.0029	0.0872	0.0018	1871	9	1789	9	1719	14	1691	34
OJ6-81	386	305	1.26	0.04974	0.00091	0.142	0.003	0.0207	0.0002	0.0066	0.0002	183	22	135	2	132	1	132	3
OJ6-82	199	2582	0.08	0.14255	0.00303	4.676	0.085	0.2379	0.0027	0.0670	0.0007	2258	38	1763	15	1376	14	1311	14
OJ6-83	243	317	0.77	0.05041	0.00137	0.184	0.005	0.0265	0.0003	0.0082	0.0004	214	38	171	4	168	2	165	7
West Cathaysia																			
S020-34	39	436	0.09	0.08975	0.00108	2.715	0.024	0.2194	0.0018	0.0648	0.0005	1420	24	1332	7	1279	9	1269	10
S020-39	124	292	0.42	0.18478	0.00190	12.907	0.113	0.5067	0.0043	0.1413	0.0012	2696	7	2673	8	2642	19	2671	21
S020-40	342	642	0.53	0.17700	0.00182	10.883	0.102	0.4458	0.0041	0.1195	0.0011	2625	7	2513	9	2377	18	2281	19
S020-42	176	503	0.35	0.08203	0.00120	1.462	0.018	0.1293	0.0011	0.0385	0.0003	1246	29	915	7	784	6	764	6
S020-43	514	2005	0.26	0.05126	0.00056	0.164	0.002	0.0232	0.0002	0.0081	0.0001	253	9	154	1	148	1	163	2
S020-45	293	604	0.49	0.06451	0.00066	0.998	0.009	0.1123	0.0009	0.0347	0.0003	758	8	703	4	686	5	690	5
S020-46	362	986	0.37	0.04985	0.00075	0.096	0.001	0.0140	0.0001	0.0049	0.0001	188	16	93	1	89	0.8	99	1
S020-47	150	226	0.66	0.07669	0.00142	1.876	0.031	0.1774	0.0015	0.0533	0.0004	1113	38	1072	11	1053	8	1049	8
S020-49	565	1875	0.30	0.06324	0.00103	0.310	0.004	0.0355	0.0003	0.0109	0.0001	716	35	274	3	225	2	219	2
S020-50	58	1345	0.04	0.04964	0.00077	0.182	0.002	0.0265	0.0003	0.0084	0.0001	178	37	169	2	169	2	169	2
S020-53	261	720	0.36	0.06405	0.00066	0.924	0.008	0.1046	0.0009	0.0362	0.0003	743	8	664	4	641	5	719	6
S020-56	182	299	0.61	0.04949	0.00200	0.166	0.006	0.0243	0.0003	0.0077	0.0001	171	95	156	6	155	2	154	1
S020-57	88	656	0.13	0.07079	0.00083	1.513	0.014	0.1551	0.0012	0.0470	0.0004	951	25	936	6	929	6	928	7
S020-58	276	483	0.57	0.05233	0.00102	0.176	0.003	0.0245	0.0003	0.0072	0.0001	300	23	164	3	156	2	144	2
S020-61	34	52	0.64	0.18858	0.00201	14.979	0.150	0.5786	0.0058	0.1408	0.0016	2730	8	2814	10	2943	24	2663	28
S020-62	142	212	0.67	0.10611	0.00127	4.006	0.045	0.2761	0.0028	0.0732	0.0012	1734	9	1635	9	1572	14	1429	23
S020-63	551	3693	0.15	0.05233	0.00056	0.175	0.002	0.0242	0.0002	0.0094	0.0001	300	9	163	1	154	1	189	2
S020-67	189	448	0.42	0.07535	0.00077	1.932	0.019	0.1873	0.0018	0.0545	0.0005	1078	9	1092	6	1107	10	1073	10
S020-72	41	62	0.66	0.07189	0.00088	1.424	0.016	0.1441	0.0013	0.0438	0.0005	983	10	899	7	868	8	867	9
S020-73	308	478	0.64	0.07626	0.00073	2.020	0.016	0.1927	0.0016	0.0560	0.0004	1102	8	1122	6	1136	9	1101	8
S020-76	161	241	0.67	0.06670	0.00069	1.219	0.011	0.1328	0.0011	0.0410	0.0003	828	8	809	5	804	6	811	7
S020-77	662	954	0.69	0.05465	0.00205	0.186	0.007	0.0247	0.0003	0.0077	0.0001	398	86	173	6	157	2	155	1
S020-79	131	126	1.04	0.15804	0.01820	0.692	0.078	0.0318	0.0008	0.0089	0.0005	2435	203	534	47	202	5	178	10
S020-82	234	1041	0.22	0.05264	0.00101	0.267	0.005	0.0368	0.0003	0.0115	0.0001	313	45	240	4	233	2	232	2
S020-86	252	242	1.04	0.10305	0.00285	3.130	0.079	0.2203	0.0025	0.0641	0.0007	1680	52	1440	19	1283	13	1256	13
S020-88	126	125	1.01	0.07133	0.00076	1.504	0.014	0.1528	0.0013	0.0459	0.0004	967	9	932	6	917	7	907	7
S020-90	162	257	0.63	0.05586	0.00070	0.505	0.006	0.0655	0.0006	0.0206	0.0002	447	12	415	4	409	4	412	4
S020-92	162	265	0.61	0.05487	0.00064	0.508	0.005	0.0672	0.0006	0.0208	0.0002	407	11	417	4	419	4	415	4
S020-95	225	557	0.40	0.16108	0.00159	10.445	0.098	0.4696	0.0045	0.1330	0.0014	2467	7	2475	9	2482	20	2524	25
S020-98	111	278	0.40	0.13152	0.00127	6.332	0.053	0.3491	0.0031	0.0988	0.0008	2118	7	2023	7	1930	15	1905	15

Table 1 (Continued)

Analysis	Th (ppm)	U (ppm)	Th/U	Ratios (common – Pb corrected)								Ages (common – Pb corrected, Ma)							
				$^{207}\text{Pb}/^{206}\text{Pb}$	$\pm 1\sigma$	$^{207}\text{Pb}/^{235}\text{U}$	$\pm 1\sigma$	$^{206}\text{Pb}/^{238}\text{U}$	$\pm 1\sigma$	$^{208}\text{Pb}/^{232}\text{Th}$	$\pm 1\sigma$	$^{207}\text{Pb}/^{206}\text{Pb}$	$\pm 1\sigma$	$^{207}\text{Pb}/^{235}\text{U}$	$\pm 1\sigma$	$^{206}\text{Pb}/^{238}\text{U}$	$\pm 1\sigma$	$^{208}\text{Pb}/^{232}\text{Th}$	$\pm 1\sigma$
S020-99	28	957	0.03	0.06863	0.00090	1.382	0.013	0.1461	0.0013	0.0444	0.0004	888	28	881	6	879	7	879	8
S020-100	114	240	0.48	0.16985	0.00301	10.949	0.153	0.4675	0.0051	0.1295	0.0014	2556	30	2519	13	2473	22	2462	26
S020-101	301	786	0.38	0.10924	0.00109	4.055	0.037	0.2693	0.0025	0.0747	0.0008	1787	8	1645	7	1537	13	1456	16
S020-114	149	276	0.54	0.07143	0.00077	1.561	0.016	0.1585	0.0015	0.0496	0.0005	970	9	955	6	949	9	979	10
S021-2	324	1101	0.29	0.05255	0.00157	0.188	0.005	0.0260	0.0003	0.0081	0.0001	310	70	175	4	165	2	164	2
S021-3	249	6216	0.04	0.05722	0.00134	0.283	0.006	0.0359	0.0004	0.0112	0.0005	500	53	253	5	227	3	224	10
S021-4	76	274	0.28	0.05798	0.00094	0.657	0.011	0.0824	0.0010	0.0378	0.0012	529	17	513	7	511	6	750	23
S021-5	221	1702	0.13	0.11019	0.00206	2.333	0.034	0.1535	0.0018	0.0444	0.0008	1803	35	1222	10	921	10	878	15
S021-6	235	272	0.86	0.06612	0.00085	1.432	0.020	0.1574	0.0019	0.0571	0.0017	810	13	903	8	943	10	1122	33
S021-9	510	1494	0.34	0.04758	0.00062	0.166	0.002	0.0253	0.0003	0.0090	0.0002	78	15	156	2	161	2	181	5
S021-10	154	365	0.42	0.08310	0.00087	2.660	0.030	0.2320	0.0026	0.0802	0.0014	1272	10	1317	8	1345	13	1558	26
S021-11	826	1290	0.64	0.04893	0.00064	0.176	0.002	0.0260	0.0003	0.0093	0.0003	144	15	164	2	166	2	188	6
S021-12	230	517	0.44	0.05044	0.00070	0.181	0.003	0.0260	0.0003	0.0099	0.0002	215	15	169	2	166	2	199	4
S021-13	195	2590	0.08	0.17084	0.00267	9.403	0.106	0.3992	0.0043	0.1105	0.0012	2566	27	2378	10	2165	20	2119	23
S021-15	96	544	0.18	0.04902	0.00105	0.167	0.003	0.0247	0.0003	0.0078	0.0001	149	51	157	3	157	2	158	2
S021-16	586	2408	0.24	0.04940	0.00108	0.169	0.003	0.0248	0.0003	0.0078	0.0001	167	52	158	3	158	2	158	2
S021-17	256	773	0.33	0.07121	0.00144	1.618	0.027	0.1647	0.0019	0.0499	0.0006	963	42	977	10	983	11	984	11
S021-18	484	1152	0.42	0.05937	0.00167	0.194	0.005	0.0237	0.0003	0.0073	0.0001	581	62	180	4	151	2	148	2
S021-19	421	2287	0.18	0.05155	0.00053	0.256	0.003	0.0361	0.0004	0.0114	0.0001	266	12	232	2	228	3	229	2
S021-20	2632	6583	0.40	0.05527	0.00146	0.189	0.004	0.0248	0.0003	0.0077	0.0001	423	60	176	4	158	2	156	2
S021-21	58	390	0.15	0.11291	0.00113	5.001	0.056	0.3213	0.0037	0.0822	0.0009	1847	9	1819	9	1796	18	1597	16
S021-22	292	538	0.54	0.07077	0.00071	1.555	0.018	0.1594	0.0018	0.0420	0.0004	951	11	953	7	954	10	831	7
S021-23	292	1596	0.18	0.05870	0.00117	0.301	0.005	0.0373	0.0004	0.0115	0.0001	556	45	268	4	236	3	232	3
S021-24	115	339	0.34	0.07071	0.00074	1.583	0.019	0.1624	0.0019	0.0416	0.0004	949	11	964	7	970	11	824	8
S021-25	446	1331	0.34	0.07545	0.00229	0.263	0.007	0.0253	0.0004	0.0076	0.0001	1080	62	237	6	161	2	153	3
S021-26	392	1797	0.22	0.05376	0.00057	0.277	0.003	0.0374	0.0004	0.0109	0.0001	361	12	248	3	237	3	220	2
S021-27	223	432	0.52	0.07921	0.00290	0.265	0.009	0.0243	0.0003	0.0073	0.0001	1177	74	239	7	155	2	146	3
S021-28A	205	342	0.60	0.05227	0.00088	0.182	0.003	0.0253	0.0003	0.0078	0.0001	297	19	170	3	161	2	157	2
S021-29	80	348	0.23	0.06570	0.00072	1.192	0.015	0.1317	0.0016	0.0378	0.0004	797	12	797	7	797	9	749	8
S021-31	134	238	0.56	0.05648	0.00081	0.529	0.008	0.0680	0.0009	0.0207	0.0003	471	15	431	5	424	5	414	5
S021-32	1511	10012	0.15	0.05511	0.00105	0.179	0.003	0.0236	0.0003	0.0074	0.0001	417	44	167	2	150	2	148	2
S021-34	908	3946	0.23	0.05444	0.00111	0.177	0.003	0.0235	0.0003	0.0074	0.0001	389	47	165	2	150	2	148	2
S021-36	302	4187	0.07	0.06455	0.00146	0.340	0.006	0.0382	0.0005	0.0117	0.0005	760	49	297	5	242	3	235	10
S021-38	657	1577	0.42	0.05306	0.00063	0.188	0.003	0.0257	0.0003	0.0078	0.0001	331	14	175	2	164	2	157	2
S021-39	21	66	0.33	0.06967	0.00135	1.483	0.029	0.1543	0.0021	0.0437	0.0011	919	20	923	12	925	12	864	21
S021-41	715	1632	0.44	0.05563	0.00068	0.194	0.003	0.0253	0.0003	0.0081	0.0001	438	14	180	2	161	2	162	2
S021-42	175	187	0.93	0.06868	0.00258	0.358	0.012	0.0378	0.0006	0.0115	0.0002	889	79	311	9	239	3	231	3
S021-43	98	1111	0.09	0.07156	0.00073	1.611	0.020	0.1633	0.0021	0.0433	0.0005	973	12	974	8	975	11	858	10
S021-45	356	1085	0.33	0.05272	0.00063	0.179	0.002	0.0247	0.0003	0.0075	0.0001	317	14	168	2	157	2	150	2
S021-46	358	2039	0.18	0.05228	0.00055	0.268	0.003	0.0371	0.0005	0.0109	0.0001	298	13	241	3	235	3	219	2
S021-47	24	784	0.03	0.09233	0.00093	3.244	0.040	0.2549	0.0032	0.0675	0.0012	1474	11	1468	10	1463	16	1319	23
S021-48	1364	9078	0.15	0.05074	0.00094	0.174	0.002	0.0249	0.0003	0.0079	0.0001	229	44	163	2	159	2	158	2
S021-49	324	541	0.60	0.08298	0.00085	2.489	0.031	0.2176	0.0027	0.0567	0.0005	1269	11	1269	9	1269	14	1115	9
S021-50	138	497	0.28	0.05097	0.00089	0.264	0.005	0.0375	0.0005	0.0108	0.0002	239	20	238	4	237	3	217	4
S021-51	383	3008	0.13	0.05067	0.00056	0.263	0.003	0.0376	0.0005	0.0103	0.0001	226	14	237	3	238	3	206	3
S021-52	2153	805	2.68	0.07239	0.00089	0.373	0.005	0.0374	0.0005	0.0101	0.0001	997	13	322	4	237	3	203	2
S021-53	368	838	0.44	0.05096	0.00066	0.179	0.003	0.0255	0.0003	0.0073	0.0001	239	15	167	2	162	2	146	2

S021-57	316	524	0.60	0.05061	0.00074	0.174	0.003	0.0250	0.0003	0.0073	0.0001	223	17	163	2	159	2	148	2
S021-59	238	365	0.65	0.05209	0.00089	0.182	0.003	0.0253	0.0003	0.0072	0.0001	289	20	169	3	161	2	144	2
S021-60	522	1015	0.51	0.05706	0.00104	0.199	0.004	0.0253	0.0004	0.0079	0.0001	494	20	184	3	161	2	159	3
S021-64	292	804	0.36	0.05077	0.00068	0.172	0.003	0.0246	0.0003	0.0071	0.0001	230	15	162	2	157	2	142	2
S021-65	150	318	0.47	0.09279	0.00416	0.327	0.014	0.0256	0.0004	0.0075	0.0002	1484	87	287	10	163	3	151	4
S021-66	258	894	0.29	0.05078	0.00077	0.261	0.004	0.0372	0.0005	0.0103	0.0002	231	18	235	3	236	3	208	3
S021-67	617	1031	0.60	0.05904	0.00061	0.754	0.009	0.0927	0.0011	0.0258	0.0002	569	12	571	5	571	7	515	4
S021-68	860	1504	0.57	0.05878	0.00151	0.200	0.005	0.0246	0.0003	0.0076	0.0001	559	57	185	4	157	2	153	2
S021-70	134	142	0.94	0.07339	0.00095	1.631	0.023	0.1611	0.0020	0.0462	0.0005	1025	13	982	9	963	11	913	10
S021-71	17	712	0.02	0.05962	0.00064	0.771	0.010	0.0938	0.0011	0.0288	0.0006	590	12	581	6	578	7	573	12
S021-72	458	2239	0.20	0.16169	0.00162	8.321	0.099	0.3732	0.0044	0.0663	0.0006	2473	9	2267	11	2045	21	1297	11
SY01-02	287	1052	0.27	0.05928	0.00186	0.590	0.017	0.0722	0.0009	0.0223	0.0003	577	70	471	11	449	5	446	7
SY01-04	194	516	0.38	0.06066	0.00080	0.724	0.010	0.0867	0.0010	0.0352	0.0005	627	29	553	6	536	6	699	9
SY01-05	443	1072	0.41	0.05329	0.00143	0.126	0.003	0.0171	0.0002	0.0054	0.0002	341	62	120	3	109	2	109	3
SY01-09	330	766	0.43	0.05354	0.00139	0.183	0.005	0.0247	0.0003	0.0080	0.0004	352	34	170	4	157	2	162	8
SY01-10	142	976	0.14	0.31580	0.00309	30.217	0.341	0.6946	0.0081	0.1789	0.0020	3550	15	3494	11	3400	31	3326	35
SY01-11	165	173	0.95	0.06844	0.00080	1.383	0.017	0.1466	0.0016	0.0474	0.0005	882	25	882	7	882	9	936	10
SY01-13	140	195	0.72	0.07786	0.00089	1.726	0.020	0.1608	0.0017	0.0491	0.0008	1143	10	1018	7	961	9	969	16
SY01-14	274	635	0.43	0.06810	0.00075	1.309	0.015	0.1394	0.0016	0.0458	0.0006	872	23	850	7	841	9	906	11
SY01-15	887	1329	0.67	0.05747	0.00087	0.581	0.009	0.0733	0.0009	0.0216	0.0007	510	16	465	6	456	6	432	14
SY01-17	111	189	0.58	0.05800	0.00115	0.594	0.012	0.0742	0.0010	0.0243	0.0005	530	44	473	7	462	6	485	9
SY01-19	135	483	0.28	0.05655	0.00101	0.203	0.004	0.0260	0.0003	0.0104	0.0002	474	40	188	3	166	2	210	4
SY01-20	282	555	0.51	0.06114	0.00066	0.520	0.006	0.0616	0.0007	0.0231	0.0003	644	24	425	4	385	4	461	5
SY01-23	571	843	0.68	0.07656	0.00075	1.944	0.020	0.1842	0.0020	0.0539	0.0006	1110	20	1097	7	1090	11	1062	11
SY01-25	100	291	0.34	0.05768	0.00086	0.581	0.009	0.0731	0.0008	0.0245	0.0004	518	33	465	6	455	5	489	8
SY01-26	68	174	0.39	0.05543	0.00086	0.327	0.005	0.0427	0.0005	0.0129	0.0002	430	35	287	4	270	3	258	4
SY01-27	413	342	1.21	0.05171	0.00100	0.111	0.002	0.0156	0.0002	0.0053	0.0001	273	45	107	2	100	1	106	1
SY01-30	670	1208	0.55	0.04807	0.00154	0.103	0.003	0.0155	0.0002	0.0049	0.0001	103	74	99	3	99	1	99	1
SY01-31	63	94	0.67	0.10611	0.00250	4.489	0.091	0.3069	0.0037	0.0891	0.0011	1734	44	1729	17	1725	18	1724	19
SY01-32	122	239	0.51	0.19119	0.00187	13.849	0.144	0.5254	0.0056	0.1509	0.0015	2752	16	2739	10	2722	24	2840	27
SY01-33	278	451	0.62	0.07005	0.00077	1.425	0.017	0.1475	0.0016	0.0505	0.0006	930	23	899	7	887	9	996	12
SY01-34	45	215	0.21	0.05240	0.00081	0.273	0.004	0.0377	0.0004	0.0123	0.0003	303	17	245	3	239	3	248	6
SY01-35	49	434	0.11	0.06896	0.00075	1.301	0.015	0.1368	0.0015	0.0530	0.0008	898	23	846	7	827	9	1043	15
SY01-36	48	584	0.08	0.07015	0.00071	1.434	0.016	0.1483	0.0016	0.0484	0.0006	933	21	903	7	891	9	956	12
SY01-37	394	1829	0.22	0.05608	0.00060	0.216	0.002	0.0280	0.0003	0.0109	0.0001	456	24	199	2	178	2	218	3
SY01-38	39	152	0.26	0.08288	0.00091	2.394	0.028	0.2094	0.0024	0.0683	0.0009	1266	22	1241	8	1226	13	1335	18
SY01-39	1822	4629	0.39	0.05522	0.00197	0.221	0.007	0.0290	0.0003	0.0090	0.0001	421	81	202	6	184	2	182	2
SY01-40	72	217	0.33	0.05858	0.00086	0.601	0.009	0.0745	0.0009	0.0266	0.0004	552	33	478	6	463	5	530	8
SY01-42	127	1036	0.12	0.06092	0.00105	0.888	0.012	0.1057	0.0012	0.0326	0.0004	636	38	645	6	648	7	648	7
SY01-43	42	123	0.34	0.05582	0.00159	0.433	0.012	0.0563	0.0007	0.0199	0.0009	445	37	365	8	353	4	398	19
SY01-45	1908	5227	0.36	0.05880	0.00164	0.262	0.007	0.0323	0.0004	0.0100	0.0001	560	62	236	5	205	2	201	2
SY01-47	279	386	0.72	0.07184	0.00094	0.723	0.010	0.0730	0.0008	0.0224	0.0005	981	12	552	6	454	5	448	10
SY01-48	50	275	0.18	0.05496	0.00075	0.503	0.007	0.0664	0.0008	0.0253	0.0005	411	31	414	5	414	5	506	9
SY01-49	124	200	0.62	0.06452	0.00338	0.241	0.012	0.0271	0.0003	0.0083	0.0001	759	113	219	10	172	2	167	2
SY01-50	430	1244	0.35	0.08009	0.00078	1.724	0.019	0.1562	0.0017	0.0456	0.0005	1199	20	1018	7	935	10	901	9
SY01-51	144	330	0.44	0.09586	0.00098	2.742	0.030	0.2074	0.0023	0.0802	0.0009	1545	20	1340	8	1215	12	1558	17
SY01-54	207	340	0.61	0.06787	0.00071	1.365	0.016	0.1458	0.0017	0.0466	0.0005	865	22	874	7	878	9	921	10

The concentrations of U and Th in each analytical spot were derived by comparison of background-corrected count rates with mean count rates on the GJ-1 standard, which has well-known concentrations of these two elements.

3.2. Hf-Isotope measurements

Hf-isotope analyses were carried out *in situ* with a New Wave Research 213 nm laser-ablation micro-probe, attached to a Nu Plasma multi-collector ICPMS at GEMOC, Macquarie University, Australia. A 5 Hz repetition rate, 30% iris setting, and energies of about 0.2 mJ/pulse were used, giving a beam diameter of ca. 50 µm. Typical ablation times were 80–120 s, resulting in pits 40–50 µm deep. The methodology and analyses of standard solutions and standard zircons are described by Griffin et al. (2000).

For the calculation of $(^{176}\text{Hf}/^{177}\text{Hf})_i$ and εHf values (Table 2), we have adopted the ^{176}Lu decay constant (1.93×10^{-11}) and the chondritic values ($^{176}\text{Lu}/^{177}\text{Hf} = 0.0332$; $^{176}\text{Hf}/^{177}\text{Hf} = 0.282772$) of Blichert-Toft and Albarède (1997). These values were reported relative to $^{176}\text{Hf}/^{177}\text{Hf} = 0.282163$ for the JMC475 standard, well within error of our previously reported value (Griffin et al., 2000, 2004). $(^{176}\text{Hf}/^{177}\text{Hf})_i$ and εHf values also have been calculated with the ^{176}Lu decay constant values of Scherer et al. (2001) and Bizzarro et al. (2003) for comparison (Table 2). To calculate model ages (T_{DM}) based on a depleted-mantle source, we have adopted a model with $(^{176}\text{Hf}/^{177}\text{Hf})_i = 0.279718$ and $^{176}\text{Lu}/^{177}\text{Hf} = 0.0384$; this produces a value of $^{176}\text{Hf}/^{177}\text{Hf}$ (0.28325) similar to that of average MORB over 4.56 Ga.

T_{DM} ages, which are calculated using the measured $^{176}\text{Lu}/^{177}\text{Hf}$ of the zircon, can only give a minimum age for the source rocks of the magma from which the zircon crystallised. Therefore, we also have calculated, for each zircon, a “crustal” model age (T_{DM}^{C}) which assumes that its parental magma was produced from an average continental crust ($^{176}\text{Lu}/^{177}\text{Hf} = 0.015$; GERM database) that originally was derived from the Depleted Mantle (Griffin et al., 2000).

4. Results

4.1. U-Pb ages

The analytical data for 383 zircons are given in Table 1. Because of counting statistics, $^{207}\text{Pb}/^{206}\text{Pb}$ ages are more precise for older zircons, while $^{206}\text{Pb}/^{238}\text{U}$ ages are more precise for younger zircons (Griffin et al.,

2004). Therefore, we use the $^{207}\text{Pb}/^{206}\text{Pb}$ ages for older (>1 Ga) zircons, and $^{206}\text{Pb}/^{238}\text{U}$ ages for younger zircons, in the following discussion. Concordia plots, age relative probability plots and weighted averages were constructed using Isoplot 2.32 (Ludwig, 2000).

4.1.1. Oujiang River

Most older zircons have rounded to sub-euhedral shapes, while all younger zircons have euhedral shape and generally larger grain size (100–150 µm). However, both older and younger zircons show weakly zoned internal structure.

Two grains give highly discordant Archean $^{207}\text{Pb}/^{206}\text{Pb}$ ages (2750–3100 Ma). Most of the discordant grains from the four samples define similar discordia lines with consistent well-defined upper intercepts (1850–1870 Ma) and similar lower (130–155 Ma) intercept ages (Fig. 2). These well-developed discordia lines are unusual in detrital zircon populations; in this case they reflect the derivation of the older populations from a relatively limited outcrop area. Because the degree of discordance is generally low, the upper intercept ages are robust with small errors, while the lower intercept ages have large errors. Another group of grains from the most upstream sample (OJ1) defines a discordia with an upper intercept of 2128 ± 120 Ma and a poorly defined lower intercept (158 ± 610 Ma).

All four samples contain concordant or near-concordant Late Mesozoic zircons (Fig. 2, insets). There is a small Indosinian age peak at 210–250 Ma, and the main clusters give Yanshanian ages (weighted mean ages of 148 ± 1.6 Ma ($n = 34$), 132 ± 1 Ma ($n = 87$) and 108 ± 2 Ma ($n = 18$), respectively). These concordant ages are consistent with the lower intercept ages defined by the discordia lines for the Paleoproterozoic populations.

The age spectra are shown in Fig. 3. Generally, two major peaks at 1850 Ma and 130–150 Ma are distinct and consistent for the four samples. In detail, from upstream (OJ1) to downstream (OJ6), the proportion of younger (<250 Ma) zircons increases (30% in OJ1, 52% in OJ3, 75% in OJ5 and 86% in OJ6). Within the Mesozoic populations, zircons with ages >140 Ma gradually decrease in abundance downstream whereas zircons with ages <130 Ma gradually increase (Fig. 2, insets). The proportion of the 1850 Ma population decreases markedly downstream, as does the 2400–2100 Ma population, which is significant in the upstream sample OJ1 but very rare in OJ5 and OJ6.

4.1.2. North River

Most of the zircons have subhedral to euhedral shapes; only the older zircons have rounded shapes. The

Table 2
Lu–Hf isotope data for detrital zircons from Cathaysia

Analysis	Age (Ma)	$^{176}\text{Hf}/^{177}\text{Hf}$	1 SE	$^{176}\text{Lu}/^{177}\text{Hf}$	$^{176}\text{Yb}/^{177}\text{Hf}$	^{176}Lu decay constant (1.93×10^{-11} and chondritic values of Blichert-Toft and Albarède (1997))						^{176}Lu decay constant (1.865×10^{-11}) of Scherer et al. (2001)			^{176}Lu decay constant (1.983×10^{-11}) of Bizzarro et al. (2003)		
						$^{176}\text{Hf}/^{177}\text{Hf}$ initial	$\varepsilon\text{Hf(t)}$	1 SE	T_{DM} (Ga)	1 SE	T_{DM}^{C} (Ga)	1 SE	$^{176}\text{Hf}/^{177}\text{Hf}$ initial	$\varepsilon\text{Hf(t)}$	1 SE	$^{176}\text{Hf}/^{177}\text{Hf}$ initial	$\varepsilon\text{Hf(t)}$
East Cathaysia																	
OJ1-01	2176	0.281535	0.000016	0.000258	0.007403	0.281524	6.25	0.56	2.28	0.02	2.35	0.04	0.281524	4.53	0.281524	7.66	
OJ1-02	131	0.282427	0.000018	0.000833	0.022701	0.282425	-9.31	0.63	1.12	0.02	1.72	0.04	0.282425	-9.40	0.282425	-9.23	
OJ1-03	1869	0.281536	0.000010	0.000862	0.024594	0.281504	-1.71	0.35	2.31	0.01	2.61	0.02	0.281505	-3.16	0.281503	-0.53	
OJ1-04	1068	0.281954	0.000014	0.001077	0.032425	0.281932	-5.28	0.49	1.77	0.02	2.21	0.03	0.281932	-6.09	0.281931	-4.62	
OJ1-06	156	0.282237	0.000033	0.001404	0.039305	0.282233	-15.53	1.16	1.40	0.05	2.12	0.07	0.282233	-15.65	0.282233	-15.44	
OJ1-07	146	0.282270	0.000017	0.000740	0.020864	0.282268	-14.52	0.60	1.33	0.02	2.05	0.04	0.282268	-14.63	0.282268	-14.43	
OJ1-08	2000	0.281555	0.000015	0.000579	0.017099	0.281532	2.37	0.53	2.27	0.02	2.46	0.03	0.281533	0.81	0.281532	3.65	
OJ1-09	2055	0.281175	0.000014	0.000623	0.018308	0.281150	-9.91	0.49	2.77	0.02	3.25	0.03	0.281151	-11.52	0.281149	-8.60	
OJ1-10	159	0.282270	0.000022	0.000666	0.016380	0.282268	-14.22	0.77	1.33	0.03	2.04	0.05	0.282268	-14.34	0.282268	-14.12	
OJ1-11	2048	0.281499	0.000013	0.001346	0.040076	0.281445	0.40	0.46	2.39	0.02	2.62	0.03	0.281447	-1.17	0.281443	1.68	
OJ1-13	136	0.282255	0.000012	0.001348	0.040830	0.282251	-15.33	0.42	1.37	0.02	2.09	0.03	0.282252	-15.43	0.282251	-15.25	
OJ1-15	147	0.282231	0.000015	0.001315	0.041603	0.282227	-15.93	0.53	1.40	0.02	2.13	0.03	0.282227	-16.04	0.282227	-15.85	
OJ1-16	1791	0.281620	0.000019	0.000857	0.024721	0.281590	-0.51	0.67	2.20	0.03	2.47	0.04	0.281591	-1.90	0.281589	0.62	
OJ1-19	1860	0.281424	0.000015	0.000703	0.022940	0.281398	-5.69	0.53	2.45	0.02	2.85	0.03	0.281399	-7.14	0.281398	-4.51	
OJ1-20	2138	0.281386	0.000016	0.000280	0.008059	0.281374	0.03	0.56	2.47	0.02	2.71	0.04	0.281375	-1.66	0.281374	1.41	
OJ1-21	1805	0.281515	0.000012	0.000801	0.025997	0.281487	-3.85	0.42	2.34	0.02	2.69	0.03	0.281488	-5.25	0.281486	-2.71	
OJ1-22	135	0.282297	0.000017	0.001128	0.037184	0.282294	-13.84	0.60	1.31	0.02	2.00	0.04	0.282294	-13.94	0.282294	-13.76	
OJ1-25	1785	0.281579	0.000021	0.000955	0.026637	0.281546	-2.23	0.74	2.26	0.03	2.58	0.05	0.281547	-3.60	0.281545	-1.11	
OJ1-26	1833	0.281550	0.000013	0.000678	0.022499	0.281526	-1.81	0.46	2.28	0.02	2.59	0.03	0.281526	-3.23	0.281525	-0.64	
OJ1-27	149	0.282284	0.000020	0.001278	0.038140	0.282280	-14.01	0.70	1.33	0.03	2.02	0.04	0.282280	-14.12	0.282280	-13.92	
OJ1-29	1800	0.281852	0.000022	0.000657	0.018531	0.281829	8.18	0.77	1.88	0.03	1.94	0.05	0.281830	6.78	0.281828	9.33	
OJ1-30	2040	0.281259	0.000019	0.000892	0.026453	0.281223	-7.66	0.67	2.68	0.02	3.10	0.04	0.281224	-9.24	0.281222	-6.37	
OJ1-31	154	0.282270	0.000017	0.001079	0.031473	0.282267	-14.38	0.60	1.34	0.02	2.05	0.04	0.282267	-14.49	0.282267	-14.28	
OJ1-35	2791	0.281030	0.000023	0.000709	0.019333	0.280991	2.00	0.81	2.97	0.03	3.09	0.05	0.280992	-0.21	0.280990	3.81	
OJ1-36	1851	0.281462	0.000014	0.000403	0.014082	0.281447	-4.16	0.49	2.38	0.02	2.74	0.03	0.281448	-5.61	0.281447	-2.98	
OJ1-38	1838	0.281408	0.000021	0.000526	0.014767	0.281389	-6.54	0.74	2.46	0.03	2.88	0.05	0.281390	-7.97	0.281388	-5.37	
OJ1-39	2060	0.281499	0.000017	0.000768	0.024088	0.281468	1.51	0.60	2.36	0.02	2.56	0.04	0.281469	-0.10	0.281467	2.82	
OJ1-40	1799	0.281544	0.000027	0.000205	0.005987	0.281537	-2.21	0.95	2.26	0.04	2.58	0.06	0.281537	-3.63	0.281537	-1.05	
OJ1-41	1869	0.281774	0.000023	0.000951	0.030652	0.281739	6.62	0.81	2.00	0.03	2.09	0.05	0.281740	5.18	0.281738	7.80	
OJ1-45	1999	0.281336	0.000015	0.000825	0.022932	0.281304	-5.77	0.53	2.57	0.02	2.96	0.03	0.281305	-7.33	0.281303	-4.51	
OJ1-46	1826	0.281415	0.000015	0.000420	0.012348	0.281400	-6.43	0.53	2.44	0.02	2.86	0.03	0.281400	-7.86	0.281400	-5.27	
OJ1-47	1850	0.281404	0.000016	0.000442	0.001749	0.281402	-5.78	0.56	2.44	0.02	2.84	0.03	0.281403	-7.24	0.281402	-4.58	
OJ1-48	1854	0.281355	0.000019	0.000567	0.016287	0.281334	-8.10	0.67	2.53	0.02	2.99	0.04	0.281335	-9.55	0.281334	-6.92	
OJ1-52	176	0.282193	0.000019	0.000771	0.028384	0.282190	-16.58	0.67	1.44	0.03	2.20	0.04	0.282190	-16.71	0.282190	-16.47	
OJ1-54	1841	0.281700	0.000019	0.000164	0.004897	0.281694	4.37	0.67	2.06	0.02	2.21	0.04	0.281694	2.91	0.281694	5.55	
OJ1-55	1846	0.281482	0.000017	0.000823	0.027801	0.281452	-4.11	0.60	2.38	0.02	2.74	0.04	0.281453	-5.54	0.281451	-2.94	
OJ1-57	2045	0.281335	0.000021	0.000833	0.026399	0.281301	-4.76	0.74	2.58	0.03	2.93	0.05	0.281303	-6.35	0.281301	-3.46	
OJ1-58	146	0.282135	0.000013	0.000981	0.031420	0.282132	-19.32	0.46	1.52	0.02	2.34	0.03	0.282132	-19.43	0.282132	-19.23	
OJ1-59	1876	0.281477	0.000012	0.000737	0.024425	0.281450	-3.48	0.42	2.38	0.02	2.72	0.03	0.281451	-4.94	0.281449	-2.29	
OJ1-60	224	0.282299	0.000017	0.000710	0.020487	0.282296	-11.76	0.60	1.29	0.02	1.94	0.04	0.282296	-11.92	0.282296	-11.62	
OJ1-61	143	0.282223	0.000016	0.000633	0.019773	0.282221	-16.24	0.56	1.39	0.02	2.15	0.03	0.282221	-16.34	0.282221	-16.15	
OJ1-62	1803	0.281631	0.000017	0.000600	0.018902	0.281610	0.47	0.60	2.17	0.02	2.42	0.04	0.281610	-0.93	0.281609	1.62	
OJ1-63	1805	0.281675	0.000040	0.000696	0.020708	0.281650	1.96	1.40	2.12	0.05	2.33	0.09	0.281651	0.56	0.281650	3.11	
OJ1-64	1828	0.281503	0.000020	0.001026	0.025226	0.281466	-4.04	0.70	2.37	0.03	2.72	0.04	0.281467	-5.44	0.281465	-2.89	

Table 2 (Continued)

Analysis	Age (Ma)	$^{176}\text{Hf}/^{177}\text{Hf}$	1 SE	$^{176}\text{Lu}/^{177}\text{Hf}$	$^{176}\text{Yb}/^{177}\text{Hf}$	^{176}Lu decay constant (1.93×10^{-11} and chondritic values of Blichert-Toft and Albarède (1997))	^{176}Lu decay constant (1.865×10^{-11}) of Scherer et al. (2001)						^{176}Lu decay constant (1.983×10^{-11}) of Bizzarro et al. (2003)			
							$^{176}\text{Hf}/^{177}\text{Hf}$ initial	$\varepsilon\text{Hf(t)}$	1 SE	T_{DM} (Ga)	1 SE	T_{DM}^{C} (Ga)	1 SE	$^{176}\text{Hf}/^{177}\text{Hf}$ initial	$\varepsilon\text{Hf(t)}$	
OJ1-65	1836	0.281450	0.000012	0.000458	0.013507	0.281433	-5.01	0.42	2.40	0.02	2.78	0.03	0.281434	-6.44	0.281433	-3.83
OJ1-66	1848	0.281264	0.000019	0.001000	0.028402	0.281228	-12.03	0.67	2.68	0.03	3.22	0.04	0.281229	-13.45	0.281227	-10.87
OJ1-67	1837	0.281492	0.000013	0.000556	0.015340	0.281472	-3.62	0.46	2.35	0.02	2.70	0.03	0.281473	-5.05	0.281471	-2.45
OJ1-69	150	0.282216	0.000014	0.001234	0.033580	0.282212	-16.39	0.49	1.42	0.02	2.16	0.03	0.282213	-16.50	0.282212	-16.30
OJ1-75	2364	0.281349	0.000014	0.000455	0.011898	0.281328	3.76	0.49	2.53	0.02	2.65	0.03	0.281329	1.88	0.281327	5.28
OJ1-76	1846	0.281499	0.000012	0.000417	0.011837	0.281484	-2.98	0.42	2.34	0.02	2.67	0.03	0.281484	-4.43	0.281483	-1.80
OJ1-78	153	0.282261	0.000010	0.001219	0.034658	0.282257	-14.73	0.35	1.36	0.01	2.07	0.02	0.282258	-14.84	0.282257	-14.64
OJ1-79	2110	0.281207	0.000017	0.000779	0.020773	0.281175	-7.73	0.60	2.74	0.02	3.16	0.04	0.281176	-9.37	0.281174	-6.39
OJ1-83	1852	0.281348	0.000014	0.000656	0.017689	0.281324	-8.51	0.49	2.55	0.02	3.01	0.03	0.281325	-9.95	0.281323	-7.34
OJ1-84	2351	0.281396	0.000013	0.000630	0.016102	0.281367	4.83	0.46	2.48	0.02	2.58	0.03	0.281368	2.98	0.281366	6.34
OJ1-85	1843	0.281496	0.000011	0.000241	0.007204	0.281487	-2.93	0.39	2.33	0.01	2.66	0.02	0.281488	-4.38	0.281487	-1.75
OJ1-87	229	0.281790	0.000018	0.000122	0.003491	0.281789	-29.56	0.63	1.94	0.02	3.01	0.04	0.281789	-29.74	0.281789	-29.42
OJ1-88	144	0.282234	0.000016	0.001179	0.037166	0.282231	-15.88	0.56	1.40	0.02	2.13	0.03	0.282231	-15.99	0.282231	-15.79
OJ1-89	248	0.282088	0.000130	0.000204	0.007984	0.282087	-18.60	4.55	1.55	0.17	2.37	0.28	0.282087	-18.79	0.282087	-18.45
OJ1-90	1848	0.281589	0.000012	0.000957	0.029013	0.281554	-0.43	0.42	2.25	0.02	2.51	0.03	0.281555	-1.86	0.281553	0.73
OJ1-91	1658	0.281658	0.000016	0.000611	0.016153	0.281638	-1.93	0.56	2.14	0.02	2.46	0.03	0.281639	-3.21	0.281638	-0.88
OJ3-01	1493	0.282121	0.000012	0.000674	0.018013	0.282101	10.64	0.42	1.53	0.02	1.55	0.03	0.282102	9.49	0.282101	11.58
OJ3-02	108	0.282405	0.000013	0.001426	0.037354	0.282402	-10.64	0.46	1.17	0.02	1.78	0.03	0.282402	-10.72	0.282402	-10.57
OJ3-04	130	0.282445	0.000018	0.001368	0.037334	0.282442	-8.74	0.63	1.11	0.02	1.69	0.04	0.282442	-8.83	0.282441	-8.66
OJ3-06	1842	0.281170	0.000017	0.000480	0.013101	0.281153	-14.84	0.60	2.77	0.02	3.39	0.04	0.281153	-16.28	0.281152	-13.67
OJ3-09	1286	0.281486	0.000016	0.000329	0.009907	0.281478	-16.31	0.56	2.35	0.02	3.05	0.03	0.281478	-17.31	0.281478	-15.50
OJ3-10	1749	0.281460	0.000014	0.000518	0.015648	0.281442	-6.75	0.49	2.39	0.02	2.82	0.03	0.281443	-8.11	0.281442	-5.63
OJ3-11	2028	0.281378	0.000012	0.000668	0.018954	0.281351	-3.39	0.42	2.51	0.02	2.83	0.03	0.281352	-4.97	0.281351	-2.10
OJ3-12	541	0.281968	0.000017	0.000063	0.001898	0.281967	-16.15	0.60	1.70	0.02	2.46	0.04	0.281967	-16.57	0.281967	-15.81
OJ3-13	127	0.282456	0.000017	0.000878	0.025344	0.282454	-8.37	0.60	1.08	0.02	1.66	0.04	0.282454	-8.47	0.282454	-8.30
OJ3-14	131	0.282518	0.000017	0.000691	0.021564	0.282516	-6.07	0.60	1.00	0.02	1.52	0.04	0.282516	-6.17	0.282516	-5.99
OJ3-15	134	0.282481	0.000020	0.002340	0.074839	0.282475	-7.47	0.70	1.09	0.03	1.61	0.04	0.282475	-7.56	0.282475	-7.39
OJ3-17	1853	0.281611	0.000016	0.000683	0.021569	0.281586	0.82	0.56	2.20	0.02	2.44	0.04	0.281587	-0.63	0.281585	1.99
OJ3-18	1851	0.281577	0.000016	0.000665	0.021782	0.281553	-0.42	0.56	2.25	0.02	2.51	0.03	0.281554	-1.85	0.281552	0.76
OJ3-19	1823	0.281360	0.000013	0.000683	0.019184	0.281336	-8.79	0.46	2.53	0.02	3.01	0.03	0.281336	-10.21	0.281335	-7.64
OJ3-22	135	0.282348	0.000013	0.001030	0.030818	0.282345	-12.03	0.46	1.24	0.02	1.89	0.03	0.282345	-12.13	0.282345	-11.95
OJ3-23	147	0.282327	0.000017	0.001348	0.036163	0.282323	-12.54	0.60	1.27	0.02	1.93	0.04	0.282323	-12.65	0.282323	-12.45
OJ3-24	127	0.282313	0.000014	0.001035	0.032229	0.282310	-13.44	0.49	1.28	0.02	1.97	0.03	0.282311	-13.54	0.282310	-13.37
OJ3-25	149	0.282304	0.000019	0.001280	0.040444	0.282300	-13.30	0.67	1.30	0.03	1.98	0.04	0.282300	-13.41	0.282300	-13.21
OJ3-26	127	0.282394	0.000017	0.001403	0.040485	0.282391	-10.61	0.60	1.19	0.02	1.80	0.04	0.282391	-10.70	0.282390	-10.54
OJ3-27	149	0.282385	0.000016	0.002008	0.068289	0.282379	-10.51	0.56	1.22	0.02	1.81	0.03	0.282379	-10.62	0.282379	-10.43
OJ3-29	2019	0.281488	0.000016	0.000734	0.021283	0.281459	0.22	0.56	2.37	0.02	2.61	0.04	0.281460	-1.36	0.281458	1.50
OJ3-30	2438	0.281331	0.000015	0.000974	0.029703	0.281284	3.97	0.53	2.59	0.02	2.70	0.03	0.281286	2.07	0.281283	5.52
OJ3-31	103	0.282531	0.000014	0.002494	0.076178	0.282526	-6.36	0.49	1.03	0.02	1.52	0.03	0.282526	-6.44	0.282526	-6.30
OJ3-32	1860	0.281297	0.000018	0.000309	0.009063	0.281286	-9.69	0.63	2.59	0.02	3.09	0.04	0.281286	-11.15	0.281285	-8.50
OJ3-33	2133	0.281466	0.000015	0.000932	0.023973	0.281427	1.78	0.53	2.41	0.02	2.60	0.03	0.281428	0.13	0.281426	3.13
OJ3-34	129	0.282432	0.000017	0.000560	0.016761	0.282431	-9.15	0.60	1.11	0.02	1.71	0.04	0.282431	-9.25	0.282431	-9.07
OJ3-35	1857	0.281573	0.000014	0.000742	0.023724	0.281546	-0.52	0.49	2.26	0.02	2.53	0.03	0.281547	-1.96	0.281545	0.66
OJ3-36	150	0.282350	0.000028	0.000738	0.021438	0.282348	-11.60	0.98	1.22	0.04	1.87	0.06	0.282348	-11.71	0.282348	-11.51
OJ3-37	128	0.282426	0.000015	0.001065	0.032665	0.282423	-9.43	0.53	1.13	0.02	1.73	0.03	0.282423	-9.52	0.282423	-9.35

OJ3-38	1820	0.281582	0.000029	0.000866	0.024371	0.281551	-1.21	1.02	2.25	0.04	2.54	0.06	0.281552	-2.61	0.281550	-0.06
OJ3-39	1744	0.281485	0.000016	0.000474	0.015308	0.281469	-5.92	0.56	2.36	0.02	2.77	0.03	0.281469	-7.28	0.281468	-4.81
OJ3-40	1867	0.281473	0.000015	0.001032	0.029122	0.281435	-4.22	0.53	2.41	0.02	2.76	0.03	0.281436	-5.65	0.281434	-3.05
OJ3-41	143	0.282221	0.000010	0.001004	0.032274	0.282218	-16.34	0.34	1.41	0.01	2.16	0.02	0.282218	-16.45	0.282218	-16.26
OJ3-42	935	0.282109	0.000014	0.001102	0.034801	0.282089	-2.78	0.49	1.56	0.02	1.95	0.03	0.282090	-3.49	0.282088	-2.21
OJ3-43	1852	0.281436	0.000010	0.000355	0.011127	0.281423	-5.00	0.35	2.41	0.01	2.80	0.02	0.281424	-6.45	0.281423	-3.81
OJ3-44	125	0.282423	0.000010	0.000810	0.024817	0.282421	-9.58	0.34	1.13	0.01	1.73	0.02	0.282421	-9.67	0.282421	-9.50
OJ3-45	134	0.282412	0.000015	0.000934	0.028260	0.282410	-9.78	0.53	1.15	0.02	1.75	0.03	0.282410	-9.88	0.282410	-9.70
OJ3-46	131	0.282422	0.000013	0.001994	0.061959	0.282417	-9.59	0.46	1.17	0.02	1.74	0.03	0.282417	-9.68	0.282417	-9.51
OJ3-47	129	0.282332	0.000013	0.000910	0.028849	0.282330	-12.72	0.46	1.25	0.02	1.93	0.03	0.282330	-12.81	0.282330	-12.64
OJ3-48	148	0.282063	0.000008	0.002350	0.082794	0.282056	-21.96	0.27	1.68	0.01	2.50	0.02	0.282057	-22.06	0.282056	-21.87
OJ3-49	129	0.282353	0.000009	0.000904	0.027385	0.282351	-11.97	0.32	1.22	0.01	1.88	0.02	0.282351	-12.07	0.282351	-11.90
OJ3-50	1868	0.281560	0.000013	0.000524	0.016994	0.281541	-0.44	0.46	2.26	0.02	2.53	0.03	0.281541	-1.90	0.281540	0.75
OJ3-51	2105	0.281440	0.000017	0.000137	0.003779	0.281434	1.38	0.60	2.39	0.02	2.60	0.04	0.281435	-0.29	0.281434	2.75
OJ3-52	156	0.282230	0.000020	0.000703	0.020252	0.282228	-15.71	0.70	1.38	0.03	2.13	0.04	0.282228	-15.82	0.282228	-15.61
OJ3-55	133	0.282419	0.000014	0.000946	0.026931	0.282417	-9.55	0.49	1.14	0.02	1.74	0.03	0.282417	-9.65	0.282417	-9.47
OJ3-56	227	0.282044	0.000016	0.001150	0.034132	0.282039	-20.78	0.56	1.65	0.02	2.49	0.03	0.282039	-20.95	0.282039	-20.64
OJ3-57	131	0.282439	0.000011	0.001818	0.054219	0.282434	-8.97	0.39	1.14	0.02	1.70	0.02	0.282435	-9.06	0.282434	-8.89
OJ3-58	108	0.282645	0.000015	0.000765	0.021068	0.282643	-2.10	0.53	0.83	0.02	1.26	0.03	0.282643	-2.18	0.282643	-2.03
OJ3-59	94	0.282636	0.000015	0.000804	0.021365	0.282635	-2.73	0.53	0.84	0.02	1.29	0.03	0.282635	-2.80	0.282635	-2.67
OJ3-61	130	0.282327	0.000014	0.000740	0.020107	0.282325	-12.86	0.49	1.25	0.02	1.93	0.03	0.282325	-12.95	0.282325	-12.78
OJ3-62	1844	0.281468	0.000011	0.000085	0.002600	0.281465	-3.70	0.39	2.36	0.01	2.71	0.02	0.281465	-5.16	0.281465	-2.51
OJ3-63	1738	0.281512	0.000017	0.000812	0.024512	0.281484	-5.51	0.60	2.34	0.02	2.74	0.04	0.281485	-6.85	0.281484	-4.41
OJ3-64	146	0.282362	0.000012	0.000555	0.014897	0.282360	-11.25	0.42	1.20	0.02	1.85	0.03	0.282360	-11.36	0.282360	-11.16
OJ3-65	409	0.282492	0.000013	0.000447	0.012121	0.282488	-0.72	0.46	1.02	0.02	1.41	0.03	0.282489	-1.03	0.282488	-0.47
OJ3-66	129	0.282489	0.000015	0.000697	0.019096	0.282487	-7.14	0.53	1.04	0.02	1.59	0.03	0.282487	-7.24	0.282487	-7.07
OJ3-67	796	0.282301	0.000013	0.000684	0.018266	0.282290	1.15	0.46	1.29	0.02	1.60	0.03	0.282291	0.54	0.282290	1.64
OJ3-68	1876	0.281523	0.000014	0.000872	0.024054	0.281491	-2.03	0.49	2.33	0.02	2.63	0.03	0.281492	-3.48	0.281490	-0.84
OJ3-69	1816	0.281479	0.000014	0.000406	0.011029	0.281465	-4.38	0.49	2.36	0.02	2.73	0.03	0.281465	-5.80	0.281464	-3.22
OJ3-70	1835	0.281550	0.000015	0.000595	0.016860	0.281529	-1.65	0.53	2.28	0.02	2.58	0.03	0.281529	-3.08	0.281528	-0.49
OJ3-71	2429	0.281112	0.000014	0.000837	0.020728	0.281072	-3.80	0.49	2.87	0.02	3.17	0.03	0.281073	-5.70	0.281071	-2.24
OJ3-73	98	0.282571	0.000019	0.001975	0.046122	0.282567	-5.02	0.67	0.96	0.03	1.43	0.04	0.282567	-5.09	0.282567	-4.96
OJ3-74	232	0.281867	0.000009	0.000081	0.002606	0.281867	-26.76	0.32	1.84	0.01	2.85	0.02	0.281867	-26.94	0.281867	-26.62
OJ3-76	127	0.282438	0.000019	0.000624	0.016773	0.282436	-8.99	0.67	1.10	0.03	1.70	0.04	0.282437	-9.08	0.282436	-8.91
OJ3-77	1850	0.281484	0.000013	0.000491	0.014264	0.281466	-3.52	0.46	2.36	0.02	2.70	0.03	0.281467	-4.96	0.281466	-2.34
OJ3-78	1849	0.281506	0.000016	0.000584	0.017633	0.281485	-2.88	0.56	2.34	0.02	2.66	0.03	0.281486	-4.32	0.281484	-1.70
OJ3-79	1860	0.281149	0.000014	0.000938	0.024871	0.281115	-15.76	0.49	2.83	0.02	3.46	0.03	0.281116	-17.20	0.281114	-14.59
OJ3-80	1852	0.281444	0.000012	0.001119	0.033320	0.281403	-5.70	0.42	2.45	0.02	2.84	0.03	0.281405	-7.12	0.281402	-4.54
OJ3-81	124	0.282351	0.000011	0.001212	0.033606	0.282348	-12.18	0.39	1.24	0.01	1.89	0.02	0.282348	-12.27	0.282348	-12.11
OJ3-82	220	0.282081	0.000020	0.000156	0.004629	0.282080	-19.47	0.70	1.56	0.03	2.40	0.04	0.282080	-19.64	0.282080	-19.34
OJ5-03	127	0.282284	0.000013	0.001402	0.036511	0.282281	-14.50	0.46	1.34	0.02	2.03	0.03	0.282281	-14.60	0.282280	-14.43
OJ5-06	136	0.282381	0.000015	0.000937	0.025529	0.282379	-10.83	0.53	1.19	0.02	1.82	0.03	0.282379	-10.93	0.282378	-10.75
OJ5-07	136	0.282408	0.000012	0.001106	0.031294	0.282405	-9.89	0.42	1.16	0.02	1.76	0.03	0.282405	-9.99	0.282405	-9.81
OJ5-08	1855	0.281531	0.000012	0.000394	0.012139	0.281517	-1.61	0.42	2.29	0.02	2.59	0.03	0.281517	-3.06	0.281516	-0.42
OJ5-09	160	0.282288	0.000016	0.001490	0.041854	0.282283	-13.65	0.56	1.33	0.02	2.01	0.03	0.282284	-13.77	0.282283	-13.56
OJ5-10	140	0.282206	0.000016	0.001152	0.034661	0.282203	-16.96	0.56	1.43	0.02	2.19	0.03	0.282203	-17.06	0.282203	-16.87
OJ5-11	128	0.282249	0.000015	0.000730	0.021828	0.282247	-15.66	0.53	1.36	0.02	2.10	0.03	0.282247	-15.76	0.282247	-15.58
OJ5-12	138	0.282262	0.000011	0.001225	0.035088	0.282259	-15.02	0.39	1.36	0.01	2.07	0.02	0.282259	-15.13	0.282259	-14.94
OJ5-13	1864	0.281495	0.000013	0.000831	0.024917	0.281465	-3.24	0.46	2.37	0.02	2.70	0.03	0.281466	-4.69	0.281464	-2.07
OJ5-14	140	0.282188	0.000014	0.000901	0.028209	0.282186	-17.57	0.49	1.45	0.02	2.23	0.03	0.282186	-17.67	0.282185	-17.48
OJ5-15	140	0.282288	0.000015	0.001137	0.033099	0.282285	-14.05	0.53	1.32	0.02	2.01	0.03	0.282285	-14.16	0.282285	-13.97

Table 2 (Continued)

Analysis	Age (Ma)	$^{176}\text{Hf}/^{177}\text{Hf}$	1 SE	$^{176}\text{Lu}/^{177}\text{Hf}$	$^{176}\text{Yb}/^{177}\text{Hf}$	^{176}Lu decay constant (1.93×10^{-11} and chondritic values of Blichert-Toft and Albarède (1997))	^{176}Lu decay constant (1.865×10^{-11}) of Scherer et al. (2001)					^{176}Lu decay constant (1.983×10^{-11}) of Bizzarro et al. (2003)				
							$^{176}\text{Hf}/^{177}\text{Hf}$ initial	$\varepsilon\text{Hf(t)}$	1 SE	T_{DM} (Ga)	1 SE	T_{DM}^{C} (Ga)	1 SE	$^{176}\text{Hf}/^{177}\text{Hf}$ initial	$\varepsilon\text{Hf(t)}$	
OJ5-16	133	0.282301	0.000014	0.001428	0.041765	0.282297	-13.77	0.49	1.31	0.02	1.99	0.03	0.282297	-13.87	0.282297	-13.69
OJ5-17	2138	0.281390	0.000014	0.001058	0.028405	0.281345	-0.99	0.49	2.52	0.02	2.77	0.03	0.281347	-2.65	0.281344	0.36
OJ5-18	2416	0.281298	0.000013	0.001077	0.031731	0.281247	2.11	0.46	2.64	0.02	2.79	0.03	0.281248	0.23	0.281245	3.64
OJ5-19	125	0.282316	0.000014	0.002054	0.061750	0.282311	-13.47	0.49	1.31	0.02	1.97	0.03	0.282311	-13.56	0.282311	-13.40
OJ5-20	148	0.282137	0.000012	0.001254	0.037090	0.282133	-19.23	0.42	1.53	0.02	2.33	0.03	0.282134	-19.34	0.282133	-19.14
OJ5-21	100	0.282677	0.000011	0.000588	0.015261	0.282676	-1.13	0.39	0.78	0.01	1.20	0.02	0.282676	-1.21	0.282676	-1.07
OJ5-22	133	0.282389	0.000018	0.001188	0.034836	0.282386	-10.64	0.63	1.19	0.02	1.80	0.04	0.282386	-10.74	0.282386	-10.56
OJ5-23	151	0.282244	0.000011	0.000927	0.027481	0.282241	-15.35	0.39	1.37	0.01	2.10	0.02	0.282241	-15.46	0.282241	-15.26
OJ5-24	132	0.282303	0.000012	0.001370	0.039194	0.282300	-13.72	0.42	1.31	0.02	1.99	0.03	0.282300	-13.82	0.282299	-13.64
OJ5-26	112	0.282667	0.000015	0.001241	0.038061	0.282664	-1.27	0.53	0.81	0.02	1.22	0.03	0.282664	-1.35	0.282664	-1.20
OJ5-28	122	0.282430	0.000016	0.002207	0.058406	0.282425	-9.51	0.56	1.16	0.02	1.73	0.03	0.282425	-9.60	0.282425	-9.44
OJ5-29	136	0.282171	0.000014	0.000963	0.029296	0.282168	-18.26	0.49	1.47	0.02	2.27	0.03	0.282169	-18.36	0.282168	-18.18
OJ5-30	224	0.282143	0.000015	0.001139	0.033420	0.282138	-17.34	0.53	1.52	0.02	2.28	0.03	0.282138	-17.51	0.282138	-17.21
OJ5-31	95	0.282567	0.000023	0.001121	0.035543	0.282565	-5.17	0.81	0.94	0.03	1.44	0.05	0.282565	-5.24	0.282565	-5.11
OJ5-33	136	0.282219	0.000010	0.001373	0.041483	0.282215	-16.60	0.34	1.42	0.01	2.17	0.02	0.282216	-16.70	0.282215	-16.52
OJ5-34	151	0.282294	0.000013	0.000832	0.024252	0.282292	-13.57	0.46	1.30	0.02	1.99	0.03	0.282292	-13.68	0.282292	-13.48
OJ5-35	1848	0.281483	0.000014	0.000846	0.026955	0.281452	-4.06	0.49	2.38	0.02	2.74	0.03	0.281453	-5.49	0.281451	-2.89
OJ5-37	155	0.282356	0.000011	0.000641	0.018819	0.282354	-11.27	0.39	1.21	0.01	1.86	0.02	0.282354	-11.38	0.282354	-11.17
OJ5-38	138	0.282403	0.000014	0.001178	0.033114	0.282400	-10.03	0.49	1.17	0.02	1.77	0.03	0.282400	-10.13	0.282400	-9.95
OJ5-39	1859	0.281321	0.000014	0.002506	0.076635	0.281229	-11.71	0.49	2.71	0.02	3.21	0.03	0.281233	-13.07	0.281227	-10.60
OJ5-41	213	0.281987	0.000017	0.000411	0.012550	0.281985	-23.00	0.60	1.69	0.02	2.61	0.04	0.281985	-23.16	0.281985	-22.86
OJ5-42	146	0.282218	0.000021	0.001329	0.036387	0.282214	-16.42	0.74	1.42	0.03	2.16	0.04	0.282214	-16.52	0.282214	-16.33
OJ5-43	133	0.282278	0.000016	0.000649	0.018758	0.282276	-14.52	0.56	1.32	0.02	2.04	0.03	0.282276	-14.62	0.282276	-14.43
OJ5-44	134	0.282392	0.000011	0.000853	0.024502	0.282390	-10.48	0.39	1.17	0.01	1.79	0.02	0.282390	-10.58	0.282390	-10.40
OJ5-46	130	0.282431	0.000014	0.000962	0.028044	0.282429	-9.20	0.49	1.12	0.02	1.71	0.03	0.282429	-9.29	0.282429	-9.12
OJ5-47	136	0.282203	0.000016	0.001035	0.030954	0.282200	-17.14	0.56	1.43	0.02	2.20	0.03	0.282200	-17.24	0.282200	-17.06
OJ5-48	2106	0.281192	0.000016	0.000167	0.004983	0.281185	-7.45	0.56	2.72	0.02	3.14	0.03	0.281185	-9.12	0.281185	-6.09
OJ5-49	133	0.282399	0.000014	0.001058	0.031641	0.282396	-10.27	0.49	1.17	0.02	1.78	0.03	0.282396	-10.37	0.282396	-10.19
OJ5-50	142	0.282208	0.000018	0.000707	0.020558	0.282206	-16.80	0.63	1.41	0.02	2.18	0.04	0.282206	-16.90	0.282206	-16.71
OJ5-51	1837	0.281474	0.000023	0.000753	0.020498	0.281447	-4.51	0.81	2.39	0.03	2.76	0.05	0.281448	-5.93	0.281446	-3.35
OJ5-52	165	0.282239	0.000014	0.001423	0.039173	0.282234	-15.27	0.49	1.40	0.02	2.11	0.03	0.282235	-15.39	0.282234	-15.17
OJ5-53	1843	0.281530	0.000013	0.000733	0.021944	0.281503	-2.36	0.46	2.31	0.02	2.63	0.03	0.281504	-3.79	0.281503	-1.19
OJ5-55	153	0.282291	0.000016	0.001115	0.029589	0.282288	-13.66	0.56	1.32	0.02	2.00	0.03	0.282288	-13.77	0.282288	-13.57
OJ5-56	1737	0.281470	0.000015	0.000605	0.017698	0.281449	-6.77	0.53	2.38	0.02	2.82	0.03	0.281450	-8.12	0.281449	-5.67
OJ5-58	128	0.282313	0.000010	0.001653	0.044891	0.282309	-13.48	0.35	1.30	0.01	1.97	0.02	0.282309	-13.57	0.282309	-13.40
OJ5-59	136	0.282275	0.000016	0.001299	0.036730	0.282272	-14.62	0.56	1.34	0.02	2.05	0.03	0.282272	-14.72	0.282271	-14.53
OJ5-60	138	0.282296	0.000016	0.000862	0.020741	0.282294	-13.79	0.56	1.30	0.02	2.00	0.03	0.282294	-13.89	0.282294	-13.70
OJ5-61	1878	0.281585	0.000010	0.000858	0.023252	0.281553	0.24	0.35	2.25	0.01	2.49	0.02	0.281554	-1.21	0.281552	1.43
OJ5-63	135	0.282386	0.000014	0.001186	0.032424	0.282383	-10.70	0.49	1.19	0.02	1.81	0.03	0.282383	-10.80	0.282383	-10.62
OJ5-64	1854	0.281369	0.000018	0.000226	0.006766	0.281361	-7.16	0.63	2.49	0.02	2.93	0.04	0.281361	-8.63	0.281361	-5.97
OJ5-66	1812	0.281494	0.000015	0.000793	0.022693	0.281466	-4.43	0.53	2.36	0.02	2.73	0.03	0.281467	-5.83	0.281465	-3.28
OJ5-67	3054	0.280842	0.000016	0.001501	0.040212	0.280751	-0.19	0.56	3.28	0.02	3.43	0.04	0.280754	-2.57	0.280748	1.75
OJ5-68	136	0.282365	0.000014	0.001412	0.039709	0.282361	-11.44	0.49	1.23	0.02	1.85	0.03	0.282361	-11.54	0.282361	-11.36
OJ5-69	141	0.282307	0.000013	0.000893	0.024012	0.282305	-13.34	0.46	1.29	0.02	1.97	0.03	0.282305	-13.44	0.282304	-13.25
OJ6-01	222	0.282080	0.000015	0.000696	0.019824	0.282077	-19.55	0.53	1.58	0.02	2.41	0.03	0.282077	-19.71	0.282077	-19.41

OJ6-02	121	0.282262	0.000018	0.000985	0.026165	0.282260	-15.38	0.63	1.35	0.02	2.08	0.04	0.282260	-15.47	0.282260	-15.30
OJ6-03	131	0.282321	0.000012	0.000945	0.024249	0.282319	-13.07	0.42	1.27	0.02	1.95	0.03	0.282319	-13.16	0.282319	-12.99
OJ6-04	135	0.282318	0.000018	0.001494	0.039318	0.282314	-13.13	0.63	1.29	0.02	1.96	0.04	0.282314	-13.23	0.282314	-13.05
OJ6-05	112	0.282624	0.000017	0.001551	0.043370	0.282621	-2.81	0.60	0.87	0.02	1.31	0.04	0.282621	-2.89	0.282621	-2.75
OJ6-06	134	0.282276	0.000014	0.000889	0.024388	0.282274	-14.59	0.49	1.33	0.02	2.04	0.03	0.282274	-14.69	0.282274	-14.50
OJ6-07	152	0.282207	0.000017	0.000824	0.023273	0.282205	-16.62	0.60	1.42	0.02	2.18	0.04	0.282205	-16.74	0.282205	-16.53
OJ6-08	106	0.282511	0.000012	0.000995	0.026459	0.282509	-6.90	0.42	1.01	0.02	1.55	0.03	0.282509	-6.98	0.282509	-6.84
OJ6-09	140	0.282188	0.000016	0.001304	0.037417	0.282184	-17.61	0.56	1.46	0.02	2.23	0.03	0.282185	-17.71	0.282184	-17.52
OJ6-10	110	0.282519	0.000015	0.001437	0.038248	0.282516	-6.56	0.53	1.01	0.02	1.54	0.03	0.282516	-6.64	0.282516	-6.50
OJ6-12	135	0.282305	0.000015	0.001240	0.035504	0.282302	-13.57	0.53	1.30	0.02	1.98	0.03	0.282302	-13.67	0.282302	-13.49
OJ6-13	133	0.282475	0.000010	0.001079	0.029002	0.282472	-7.59	0.34	1.06	0.01	1.62	0.02	0.282472	-7.68	0.282472	-7.51
OJ6-16	129	0.282376	0.000007	0.001509	0.043594	0.282372	-11.21	0.25	1.21	0.01	1.83	0.02	0.282372	-11.31	0.282372	-11.14
OJ6-17	137	0.282151	0.000012	0.000785	0.023770	0.282149	-18.93	0.42	1.49	0.02	2.31	0.03	0.282149	-19.03	0.282149	-18.85
OJ6-18	137	0.282271	0.000013	0.000834	0.023745	0.282269	-14.69	0.46	1.33	0.02	2.05	0.03	0.282269	-14.79	0.282269	-14.61
OJ6-19	113	0.282610	0.000018	0.000994	0.026236	0.282608	-3.24	0.63	0.88	0.02	1.34	0.04	0.282608	-3.33	0.282608	-3.17
OJ6-20	111	0.282584	0.000016	0.001586	0.044524	0.282581	-4.25	0.56	0.93	0.02	1.40	0.03	0.282581	-4.33	0.282581	-4.19
OJ6-21	132	0.282336	0.000010	0.001178	0.033213	0.282333	-12.53	0.35	1.26	0.01	1.92	0.02	0.282333	-12.63	0.282333	-12.45
OJ6-22	107	0.282557	0.000017	0.002124	0.059216	0.282553	-5.33	0.60	0.98	0.02	1.46	0.04	0.282553	-5.41	0.282552	-5.27
OJ6-23	128	0.282210	0.000014	0.000762	0.021499	0.282208	-17.04	0.49	1.41	0.02	2.19	0.03	0.282208	-17.14	0.282208	-16.96
OJ6-25	112	0.282574	0.000011	0.001286	0.034345	0.282571	-4.56	0.39	0.94	0.02	1.42	0.02	0.282571	-4.64	0.282571	-4.49
OJ6-26	128	0.282526	0.000013	0.002316	0.074159	0.282520	-6.00	0.46	1.03	0.02	1.52	0.03	0.282520	-6.09	0.282520	-5.93
OJ6-27	134	0.282299	0.000017	0.001298	0.036651	0.282296	-13.81	0.60	1.31	0.02	2.00	0.04	0.282296	-13.91	0.282296	-13.73
OJ6-28	96	0.282611	0.000014	0.001147	0.033360	0.282609	-3.59	0.49	0.88	0.02	1.34	0.03	0.282609	-3.66	0.282609	-3.53
OJ6-30	135	0.282201	0.000015	0.000624	0.017660	0.282199	-17.19	0.53	1.42	0.02	2.20	0.03	0.282199	-17.29	0.282199	-17.11
OJ6-31	135	0.282378	0.000019	0.000813	0.021731	0.282376	-10.95	0.67	1.19	0.03	1.82	0.04	0.282376	-11.05	0.282376	-10.87
OJ6-32	109	0.282575	0.000010	0.000946	0.025221	0.282573	-4.57	0.35	0.93	0.01	1.41	0.02	0.282573	-4.65	0.282573	-4.50
OJ6-33	123	0.282452	0.000016	0.000485	0.013617	0.282451	-8.57	0.56	1.08	0.02	1.67	0.03	0.282451	-8.66	0.282451	-8.49
OJ6-34	102	0.282547	0.000015	0.001034	0.029147	0.282545	-5.72	0.53	0.97	0.02	1.48	0.03	0.282545	-5.79	0.282545	-5.66
OJ6-35	1854	0.281507	0.000024	0.000294	0.008328	0.281496	-2.35	0.84	2.32	0.03	2.64	0.05	0.281497	-3.81	0.281496	-3.16
OJ6-36	124	0.282360	0.000015	0.001291	0.036185	0.282357	-11.87	0.53	1.23	0.02	1.87	0.03	0.282357	-11.96	0.282357	-11.80
OJ6-37	137	0.282331	0.000017	0.001315	0.036234	0.282328	-12.61	0.60	1.27	0.02	1.93	0.04	0.282328	-12.71	0.282327	-12.53
OJ6-39	109	0.282454	0.000012	0.001652	0.045983	0.282451	-8.90	0.42	1.11	0.02	1.68	0.03	0.282451	-8.98	0.282450	-8.83
OJ6-40	150	0.282125	0.000021	0.002603	0.074740	0.282117	-19.75	0.74	1.60	0.03	2.37	0.04	0.282118	-19.86	0.282117	-19.66
OJ6-41	1856	0.281444	0.000020	0.000412	0.013674	0.281429	-4.70	0.70	2.41	0.03	2.78	0.04	0.281429	-6.15	0.281429	-5.51
OJ6-42	143	0.282240	0.000013	0.001202	0.038234	0.282237	-15.69	0.46	1.39	0.02	2.12	0.03	0.282237	-15.80	0.282237	-15.61
OJ6-43	132	0.282298	0.000016	0.001604	0.051129	0.282294	-13.92	0.56	1.32	0.02	2.00	0.03	0.282294	-14.01	0.282294	-13.84
OJ6-44	128	0.282461	0.000015	0.000967	0.029927	0.282459	-8.18	0.53	1.08	0.02	1.65	0.03	0.282459	-8.28	0.282459	-8.10
OJ6-45	109	0.282470	0.000021	0.001659	0.052019	0.282467	-8.33	0.74	1.09	0.03	1.64	0.05	0.282467	-8.41	0.282466	-8.27
OJ6-47	128	0.282419	0.000014	0.001084	0.032075	0.282416	-9.68	0.49	1.14	0.02	1.74	0.03	0.282416	-9.77	0.282416	-9.60
OJ6-48	127	0.282407	0.000016	0.001550	0.048059	0.282403	-10.16	0.56	1.17	0.02	1.77	0.03	0.282403	-10.26	0.282403	-10.09
OJ6-49	135	0.282149	0.000012	0.001455	0.047542	0.282145	-19.11	0.42	1.52	0.02	2.32	0.03	0.282145	-19.21	0.282145	-19.03
OJ6-50	1868	0.281566	0.000014	0.000814	0.026305	0.281536	-0.61	0.49	2.27	0.02	2.54	0.03	0.281537	-2.05	0.281535	0.57
OJ6-51	136	0.282123	0.000014	0.001867	0.051599	0.282118	-20.05	0.49	1.57	0.02	2.37	0.03	0.282118	-20.14	0.282118	-19.97
OJ6-52	128	0.282273	0.000013	0.001051	0.031162	0.282270	-14.84	0.46	1.34	0.02	2.05	0.03	0.282270	-14.93	0.282270	-14.76
OJ6-53	126	0.282322	0.000014	0.001051	0.032898	0.282319	-13.15	0.49	1.27	0.02	1.95	0.03	0.282320	-13.24	0.282319	-13.07
OJ6-56	2092	0.281518	0.000013	0.000920	0.024878	0.281480	2.70	0.46	2.34	0.02	2.51	0.03	0.281481	1.08	0.281479	4.03
OJ6-57	141	0.282183	0.000017	0.001051	0.033107	0.282180	-17.74	0.60	1.46	0.02	2.24	0.04	0.282180	-17.84	0.282180	-17.65
OJ6-59	1857	0.281440	0.000013	0.000775	0.024689	0.281412	-5.29	0.46	2.43	0.02	2.82	0.03	0.281413	-6.72	0.281411	-4.11
OJ6-60	2370	0.281244	0.000017	0.000343	0.010155	0.281228	0.35	0.60	2.66	0.02	2.87	0.04	0.281229	-1.53	0.281228	1.89

Table 2 (Continued)

Analysis	Age (Ma)	$^{176}\text{Hf}/^{177}\text{Hf}$	1 SE	$^{176}\text{Lu}/^{177}\text{Hf}$	$^{176}\text{Yb}/^{177}\text{Hf}$	176Lu decay constant (1.93×10^{-11} and chondritic values of Blichert-Toft and Albarede (1997))							176Lu decay constant (1.865×10^{-11}) of Scherer et al. (2001)				176Lu decay constant (1.983×10^{-11}) of Bizzarro et al. (2003)	
						$^{176}\text{Hf}/^{177}\text{Hf}$	$\varepsilon\text{Hf(t)}$	1 SE	T_{DM} (Ga)	1 SE	T_{DM}^{C} (Ga)	1 SE	$^{176}\text{Hf}/^{177}\text{Hf}$	$\varepsilon\text{Hf(t)}$	1 SE	$^{176}\text{Hf}/^{177}\text{Hf}$	$\varepsilon\text{Hf(t)}$	
						initial	initial	initial	initial	initial	initial	initial	initial	initial	initial	initial	initial	
OJ6-61	1808	0.281505	0.000018	0.001195	0.036645	0.281463	-4.63	0.63	2.37	0.02	2.74	0.04	0.281464	-6.02	0.281461	-3.51		
OJ6-62	150	0.282245	0.000016	0.000820	0.023800	0.282243	-15.32	0.56	1.37	0.02	2.10	0.03	0.282243	-15.43	0.282243	-15.23		
OJ6-63	133	0.282282	0.000014	0.000797	0.024384	0.282280	-14.39	0.49	1.32	0.02	2.03	0.03	0.282280	-14.49	0.282280	-14.31		
OJ6-64	1861	0.281548	0.000016	0.000898	0.027114	0.281515	-1.52	0.56	2.30	0.02	2.59	0.03	0.281516	-2.95	0.281514	-0.34		
OJ6-65	100	0.282623	0.000017	0.000821	0.024100	0.282621	-3.06	0.60	0.86	0.02	1.32	0.04	0.282621	-3.13	0.282621	-3.00		
OJ6-66	94	0.282619	0.000018	0.001407	0.042284	0.282616	-3.37	0.63	0.88	0.02	1.33	0.04	0.282617	-3.44	0.282616	-3.31		
OJ6-67	142	0.282206	0.000012	0.000927	0.028570	0.282203	-16.89	0.42	1.42	0.02	2.19	0.03	0.282204	-16.99	0.282203	-16.80		
OJ6-69	129	0.282326	0.000019	0.000910	0.026120	0.282324	-12.93	0.67	1.26	0.03	1.94	0.04	0.282324	-13.03	0.282324	-12.85		
OJ6-70	137	0.282275	0.000014	0.000704	0.020151	0.282273	-14.54	0.49	1.32	0.02	2.04	0.03	0.282273	-14.64	0.282273	-14.45		
OJ6-71	126	0.282321	0.000013	0.001555	0.049288	0.282317	-13.23	0.46	1.29	0.02	1.95	0.03	0.282317	-13.32	0.282317	-13.15		
OJ6-73	131	0.282386	0.000013	0.000913	0.026660	0.282384	-10.76	0.46	1.18	0.02	1.81	0.03	0.282384	-10.86	0.282384	-10.68		
OJ6-74	132	0.282425	0.000014	0.001121	0.031956	0.282422	-9.38	0.49	1.13	0.02	1.73	0.03	0.282422	-9.48	0.282422	-9.30		
OJ6-75	112	0.282554	0.000015	0.001038	0.028861	0.282552	-5.25	0.53	0.96	0.02	1.46	0.03	0.282552	-5.33	0.282552	-5.18		
OJ6-76	133	0.282455	0.000020	0.001075	0.030108	0.282452	-8.29	0.70	1.09	0.03	1.66	0.04	0.282452	-8.39	0.282452	-8.21		
OJ6-77	130	0.282436	0.000011	0.000794	0.023448	0.282434	-9.01	0.39	1.11	0.01	1.70	0.02	0.282434	-9.10	0.282434	-8.93		
OJ6-78	126	0.282219	0.000015	0.000649	0.018147	0.282217	-16.76	0.53	1.40	0.02	2.17	0.03	0.282217	-16.85	0.282217	-16.68		
OJ6-79	130	0.282345	0.000014	0.000857	0.024183	0.282343	-12.23	0.49	1.23	0.02	1.90	0.03	0.282343	-12.33	0.282343	-12.15		
OJ6-80	1871	0.281584	0.000013	0.001216	0.037303	0.281539	-0.42	0.46	2.27	0.02	2.53	0.03	0.281541	-1.86	0.281538	0.74		
OJ6-81	132	0.282315	0.000015	0.001413	0.039071	0.282311	-13.30	0.53	1.29	0.02	1.96	0.03	0.282312	-13.39	0.282311	-13.22		
OJ6-82	2258	0.281303	0.000017	0.001017	0.025699	0.281258	-1.26	0.60	2.63	0.02	2.88	0.04	0.281259	-3.01	0.281256	0.17		
OJ6-83	168	0.282174	0.000013	0.000544	0.015917	0.282172	-17.40	0.46	1.45	0.02	2.24	0.03	0.282172	-17.53	0.282172	-17.30		
West Cathaysia																		
S020-34	1420	0.281626	0.000017	0.000627	0.034393	0.281609	-8.55	0.60	2.18	0.02	2.68	0.04	0.281609	-9.64	0.281608	-7.66		
S020-39	2696	0.281036	0.000011	0.000664	0.033982	0.281001	0.06	0.39	2.95	0.01	3.14	0.02	0.281002	-2.07	0.281000	1.81		
S020-40	2625	0.281209	0.000010	0.001072	0.054343	0.281153	3.79	0.35	2.76	0.01	2.85	0.02	0.281155	1.74	0.281152	5.47		
S020-42	1246	0.282281	0.000011	0.000542	0.026135	0.282268	10.78	0.39	1.31	0.01	1.35	0.02	0.282268	9.82	0.282267	11.56		
S020-43	148	0.282507	0.000011	0.001308	0.058165	0.282503	-6.15	0.39	1.03	0.02	1.54	0.02	0.282503	-6.26	0.282503	-6.06		
S020-45	686	0.282618	0.000019	0.003002	0.189982	0.282578	8.80	0.67	0.92	0.03	1.04	0.04	0.282579	8.32	0.282577	9.20		
S020-46	89	0.282499	0.000009	0.000999	0.043712	0.282497	-7.69	0.33	1.03	0.01	1.59	0.02	0.282497	-7.76	0.282497	-7.64		
S020-47	1113	0.281937	0.000011	0.000549	0.026876	0.281925	-4.47	0.39	1.77	0.01	2.19	0.02	0.281925	-5.32	0.281925	-3.77		
S020-49	225	0.282251	0.000011	0.000950	0.045212	0.282247	-13.47	0.39	1.36	0.01	2.05	0.02	0.282247	-13.64	0.282247	-13.33		
S020-50	169	0.282391	0.000009	0.001294	0.065695	0.282387	-9.79	0.33	1.19	0.01	1.78	0.02	0.282387	-9.92	0.282387	-9.69		
S020-53	641	0.282229	0.000012	0.000728	0.037063	0.282220	-4.92	0.42	1.39	0.02	1.85	0.03	0.282220	-5.40	0.282220	-4.52		
S020-56	155	0.282653	0.000015	0.001249	0.061132	0.282649	-0.82	0.53	0.83	0.02	1.22	0.03	0.282649	-0.94	0.282649	-0.73		
S020-57	929	0.282279	0.000014	0.000495	0.027586	0.282270	3.50	0.49	1.31	0.02	1.56	0.03	0.282270	2.78	0.282270	4.08		
S020-58	156	0.282689	0.000012	0.001151	0.053811	0.282686	0.48	0.42	0.77	0.02	1.14	0.03	0.282686	0.37	0.282685	0.58		
S020-61	2730	0.280962	0.000015	0.000591	0.029083	0.280930	-1.63	0.53	3.04	0.02	3.27	0.03	0.280931	-3.80	0.280929	0.14		
S020-62	1734	0.282095	0.000013	0.001930	0.107301	0.282029	13.75	0.46	1.62	0.02	1.55	0.03	0.282032	12.45	0.282027	14.81		
S020-63	154	0.282461	0.000011	0.001405	0.074219	0.282457	-7.65	0.39	1.09	0.02	1.64	0.02	0.282457	-7.77	0.282457	-7.56		
S020-67	1078	0.282028	0.000011	0.000902	0.051882	0.282009	-2.30	0.39	1.66	0.01	2.03	0.02	0.282010	-3.12	0.282009	-1.64		
S020-72	868	0.282350	0.000013	0.000501	0.022188	0.282342	4.62	0.46	1.22	0.02	1.44	0.03	0.282342	3.96	0.282341	5.16		
S020-73	1102	0.282232	0.000014	0.001045	0.046989	0.282210	5.36	0.49	1.39	0.02	1.58	0.03	0.282210	4.53	0.282209	6.04		
S020-76	804	0.281962	0.000013	0.000479	0.024096	0.281955	-10.57	0.46	1.73	0.02	2.32	0.03	0.281955	-11.18	0.281954	-10.07		
S020-77	157	0.282606	0.000010	0.001167	0.051794	0.282602	-2.43	0.34	0.89	0.01	1.32	0.02	0.282603	-2.55	0.282602	-2.34		

S020-82	233	0.282444	0.000014	0.000490	0.027411	0.282442	-6.39	0.49	1.09	0.02	1.62	0.03	0.282442	-6.57	0.282442	-6.25
S020-86	1680	0.281531	0.000013	0.000824	0.046518	0.281504	-6.18	0.46	2.32	0.02	2.74	0.03	0.281505	-7.47	0.281503	-5.12
S020-88	917	0.282087	0.000014	0.000375	0.020474	0.282080	-3.50	0.49	1.56	0.02	1.98	0.03	0.282081	-4.21	0.282080	-2.93
S020-90	409	0.282282	0.000020	0.001359	0.075270	0.282271	-8.41	0.70	1.34	0.03	1.88	0.04	0.282272	-8.71	0.282271	-8.17
S020-92	419	0.282327	0.000013	0.001056	0.055141	0.282318	-6.51	0.46	1.27	0.02	1.78	0.03	0.282319	-6.83	0.282318	-6.26
S020-95	2467	0.281340	0.000011	0.000805	0.035830	0.281301	5.26	0.39	2.57	0.01	2.64	0.02	0.281302	3.32	0.281300	6.84
S020-98	2118	0.281172	0.000012	0.000169	0.008469	0.281165	-7.88	0.42	2.74	0.02	3.18	0.03	0.281165	-9.56	0.281165	-6.51
S020-99	879	0.281811	0.000013	0.000840	0.037076	0.281797	-14.43	0.46	1.95	0.02	2.62	0.03	0.281797	-15.10	0.281796	-13.89
S020-100	2556	0.281028	0.000014	0.000506	0.026481	0.281002	-3.23	0.49	2.95	0.02	3.23	0.03	0.281003	-5.26	0.281002	-1.57
S020-101	1787	0.281760	0.000016	0.000581	0.031730	0.281740	4.71	0.56	2.00	0.02	2.15	0.04	0.281740	3.32	0.281739	5.85
S020-114	949	0.281945	0.000016	0.000429	0.019446	0.281937	-7.84	0.56	1.75	0.02	2.27	0.03	0.281937	-8.57	0.281937	-7.25
S-021-2	165	0.282465	0.000010	0.001475	0.056823	0.282460	-7.28	0.33	1.09	0.01	1.62	0.02	0.282460	-7.40	0.282460	-7.18
S-021-3	227	0.282417	0.000011	0.003946	0.164107	0.282400	-8.02	0.39	1.24	0.02	1.72	0.02	0.282400	-8.17	0.282399	-7.89
S-021-4	511	0.281872	0.000023	0.001478	0.053966	0.281857	-20.73	0.81	1.90	0.03	2.71	0.05	0.281858	-21.11	0.281857	-20.43
S-021-5	1803	0.281194	0.000010	0.001126	0.044943	0.281154	-15.70	0.35	2.78	0.01	3.41	0.02	0.281155	-17.08	0.281153	-14.58
S-021-6	943	0.282135	0.000009	0.000308	0.011831	0.282129	-1.17	0.30	1.49	0.01	1.86	0.02	0.282130	-1.89	0.282129	-0.57
S-021-9	161	0.282570	0.000011	0.002037	0.081246	0.282564	-3.72	0.39	0.96	0.02	1.40	0.02	0.282564	-3.83	0.282563	-3.62
S-021-10	1272	0.281811	0.000013	0.000970	0.039881	0.281787	-5.67	0.46	1.95	0.02	2.39	0.03	0.281788	-6.64	0.281786	-4.88
S-021-11	166	0.282469	0.000011	0.001263	0.053113	0.282465	-7.09	0.39	1.08	0.02	1.61	0.02	0.282465	-7.22	0.282465	-6.99
S-021-12	166	0.282499	0.000010	0.000819	0.031931	0.282496	-5.98	0.35	1.03	0.01	1.55	0.02	0.282496	-6.11	0.282496	-5.88
S-021-13	2566	0.281154	0.000009	0.001726	0.074796	0.281066	-0.71	0.33	2.88	0.01	3.08	0.02	0.281069	-2.67	0.281064	0.89
S-021-15	157	0.282542	0.000010	0.000853	0.033487	0.282539	-4.66	0.34	0.97	0.01	1.46	0.02	0.282539	-4.78	0.282539	-4.57
S-021-16	158	0.282429	0.000010	0.000988	0.038435	0.282426	-8.65	0.34	1.12	0.01	1.70	0.02	0.282426	-8.77	0.282426	-8.56
S-021-17	983	0.282330	0.000010	0.001933	0.060554	0.282293	5.56	0.35	1.29	0.01	1.47	0.02	0.282294	4.84	0.282292	6.15
S-021-18	151	0.282412	0.000013	0.001863	0.078121	0.282407	-9.50	0.46	1.17	0.02	1.75	0.03	0.282407	-9.61	0.282406	-9.41
S-021-19	228	0.282368	0.000009	0.001327	0.045989	0.282362	-9.32	0.31	1.22	0.01	1.80	0.02	0.282362	-9.49	0.282362	-9.18
S-021-20	423	0.282466	0.000014	0.002382	0.079770	0.282446	-1.89	0.49	1.12	0.02	1.50	0.03	0.282447	-2.19	0.282446	-1.64
S-021-21	1847	0.281960	0.000017	0.000760	0.028457	0.281932	12.97	0.60	1.75	0.02	1.68	0.04	0.281933	11.54	0.281932	14.14
S-021-22	954	0.282056	0.000011	0.000278	0.011047	0.282051	-3.69	0.39	1.60	0.01	2.02	0.02	0.282051	-4.43	0.282051	-3.09
S-021-23	236	0.282338	0.000013	0.000572	0.023627	0.282335	-10.09	0.46	1.23	0.02	1.85	0.03	0.282335	-10.26	0.282335	-9.94
S-021-24	970	0.282212	0.000010	0.000596	0.022128	0.282201	1.99	0.35	1.40	0.01	1.68	0.02	0.282201	1.25	0.282200	2.59
S-021-25	161	0.282509	0.000014	0.002675	0.086799	0.282501	-5.94	0.49	1.06	0.02	1.54	0.03	0.282501	-6.06	0.282500	-5.85
S-021-26	237	0.282396	0.000013	0.000824	0.033531	0.282392	-8.05	0.46	1.16	0.02	1.73	0.03	0.282392	-8.23	0.282392	-7.91
S-021-27	155	0.282594	0.000008	0.001293	0.043513	0.282590	-2.92	0.26	0.91	0.01	1.35	0.02	0.282590	-3.03	0.282590	-2.82
S-021-28	161	0.282559	0.000012	0.000706	0.029043	0.282557	-3.96	0.42	0.94	0.02	1.42	0.03	0.282557	-4.08	0.282557	-3.86
S-021-29	797	0.281321	0.000013	0.000353	0.010675	0.281316	-33.37	0.46	2.56	0.02	3.68	0.03	0.281316	-33.98	0.281315	-32.87
S-021-31	424	0.282320	0.000009	0.001177	0.037624	0.282310	-6.69	0.31	1.28	0.01	1.79	0.02	0.282311	-7.00	0.282310	-6.43
S-021-32	150	0.282462	0.000010	0.002716	0.117978	0.282454	-7.84	0.35	1.13	0.01	1.65	0.02	0.282454	-7.95	0.282454	-7.75
S-021-34	150	0.282409	0.000014	0.001634	0.058568	0.282404	-9.60	0.49	1.17	0.02	1.75	0.03	0.282404	-9.71	0.282404	-9.52
S-021-36	242	0.282328	0.000012	0.002099	0.062314	0.282318	-10.56	0.42	1.30	0.02	1.88	0.03	0.282319	-10.73	0.282318	-10.42
S-021-38	164	0.282453	0.000015	0.002202	0.068494	0.282446	-7.81	0.53	1.13	0.02	1.66	0.03	0.282446	-7.93	0.282446	-7.71
S-021-39	925	0.282430	0.000010	0.000646	0.024902	0.282418	8.66	0.35	1.11	0.01	1.24	0.02	0.282419	7.95	0.282418	9.24
S-021-41	161	0.282456	0.000009	0.001293	0.044893	0.282452	-7.67	0.32	1.10	0.01	1.64	0.02	0.282452	-7.78	0.282452	-7.57
S-021-42	239	0.282475	0.000013	0.001038	0.036126	0.282470	-5.25	0.46	1.06	0.02	1.56	0.03	0.282470	-5.42	0.282470	-5.10
S-021-43	975	0.282001	0.000012	0.001630	0.051208	0.281970	-6.07	0.42	1.73	0.02	2.18	0.03	0.281971	-6.79	0.281969	-5.48
S-021-45	157	0.282469	0.000014	0.000872	0.034276	0.282466	-7.25	0.49	1.07	0.02	1.62	0.03	0.282466	-7.37	0.282466	-7.15
S-021-46	235	0.282308	0.000010	0.001531	0.050395	0.282301	-11.32	0.35	1.31	0.01	1.92	0.02	0.282301	-11.50	0.282301	-11.18
S-021-47	1474	0.281611	0.000014	0.000320	0.009149	0.281602	-7.53	0.49	2.18	0.02	2.66	0.03	0.281602	-8.68	0.281602	-6.59
S-021-48	159	0.282411	0.000014	0.002772	0.089621	0.282402	-9.46	0.49	1.21	0.02	1.75	0.03	0.282403	-9.57	0.282402	-9.37
S-021-49	1269	0.281958	0.000009	0.000867	0.030058	0.281937	-0.44	0.32	1.75	0.01	2.07	0.02	0.281937	-1.41	0.281936	0.35
S-021-50	237	0.282329	0.000010	0.001222	0.036961	0.282323	-10.49	0.35	1.27	0.01	1.87	0.02	0.282324	-10.66	0.282323	-10.34
S-021-51	238	0.282329	0.000011	0.001123	0.034895	0.282324	-10.45	0.39	1.26	0.01	1.87	0.02	0.282324	-10.63	0.282324	-10.31
S-021-52	237	0.282432	0.000013	0.002100	0.080995	0.282422	-6.99	0.46	1.15	0.02	1.66	0.03	0.282423	-7.16	0.282422	-6.85

Table 2 (Continued)

Analysis	Age (Ma)	$^{176}\text{Hf}/^{177}\text{Hf}$	1 SE	$^{176}\text{Lu}/^{177}\text{Hf}$	$^{176}\text{Yb}/^{177}\text{Hf}$	^{176}Lu decay constant (1.93×10^{-11} and chondritic values of Blöcher-Toft and Albarède (1997))						^{176}Lu decay constant (1.865×10^{-11}) of Scherer et al. (2001)	^{176}Lu decay constant (1.983×10^{-11}) of Bizzarro et al. (2003)	
		$^{176}\text{Hf}/^{177}\text{Hf}$	$\epsilon\text{Hf(t)}$	1 SE	T_{DM} (Ga)	1 SE	T_{DM}^{C} (Ga)	1 SE	$^{176}\text{Hf}/^{177}\text{Hf}$	$\epsilon\text{Hf(t)}$	1 SE	$^{176}\text{Hf}/^{177}\text{Hf}$	$\epsilon\text{Hf(t)}$	
		initial	initial	initial	initial	initial	initial	initial	initial	initial	initial	initial	initial	
S-021-53	162	0.282485	0.000011	0.000757	0.028485	0.282483	-6.56	0.39	1.04	0.01	1.58	0.02	0.282483	-6.68
S-021-57	159	0.282468	0.000013	0.001311	0.042697	0.282464	-7.29	0.46	1.08	0.02	1.62	0.03	0.282464	-7.40
S-021-59	161	0.282427	0.000010	0.001266	0.042124	0.282423	-8.69	0.35	1.14	0.01	1.71	0.02	0.282423	-8.81
S-021-60	161	0.282436	0.000013	0.002826	0.092544	0.282427	-8.54	0.46	1.17	0.02	1.70	0.03	0.282428	-8.66
S-021-64	157	0.282441	0.000009	0.001163	0.040334	0.282437	-8.27	0.33	1.11	0.01	1.68	0.02	0.282438	-8.39
S-021-65	163	0.282493	0.000012	0.001310	0.054960	0.282489	-6.32	0.42	1.05	0.02	1.56	0.03	0.282489	-6.44
S-021-66	236	0.282321	0.000012	0.001282	0.039181	0.282315	-10.80	0.42	1.28	0.02	1.89	0.03	0.282315	-10.98
S-021-67	571	0.282326	0.000012	0.001224	0.043866	0.282312	-3.25	0.42	1.27	0.02	1.69	0.03	0.282313	-3.67
S-021-68	157	0.282470	0.000012	0.001107	0.039906	0.282467	-7.24	0.42	1.07	0.02	1.62	0.03	0.282467	-7.35
S-021-70	963	0.282199	0.000012	0.001507	0.053771	0.282171	0.76	0.42	1.46	0.02	1.75	0.03	0.282172	0.05
S-021-71	578	0.281620	0.000014	0.000598	0.021608	0.281613	-27.84	0.49	2.19	0.02	3.18	0.03	0.281614	-28.28
S-021-72	2473	0.280949	0.000010	0.000771	0.028350	0.280911	-8.45	0.35	3.08	0.01	3.49	0.02	0.280913	-10.39
SY01-02	449	0.282138	0.000012	0.002272	0.074319	0.282118	-12.91	0.42	1.57	0.02	2.19	0.03	0.282119	-13.24
SY01-04	536	0.282417	0.000011	0.002036	0.057212	0.282396	-1.10	0.39	1.17	0.02	1.54	0.02	0.282397	-1.48
SY01-05	109	0.282527	0.000011	0.000903	0.025050	0.282525	-6.26	0.39	0.99	0.01	1.52	0.02	0.282525	-6.34
SY01-09	157	0.282559	0.000041	0.001116	0.035345	0.282556	-4.09	1.44	0.95	0.06	1.42	0.09	0.282556	-4.21
SY01-10	3550	0.280526	0.000016	0.000629	0.018068	0.280481	2.28	0.56	3.61	0.02	3.65	0.04	0.280483	-0.59
SY01-11	882	0.282490	0.000016	0.000933	0.025036	0.282474	9.64	0.56	1.04	0.02	1.14	0.04	0.282475	8.97
SY01-13	1143	0.282222	0.000016	0.000979	0.030421	0.282200	5.98	0.56	1.40	0.02	1.57	0.04	0.282201	5.11
SY01-14	841	0.282217	0.000015	0.001718	0.053670	0.282189	-1.41	0.53	1.44	0.02	1.79	0.03	0.282190	-2.03
SY01-17	462	0.282357	0.000012	0.002033	0.060138	0.282339	-4.81	0.42	1.26	0.02	1.71	0.03	0.282339	-5.14
SY01-19	166	0.282526	0.000021	0.000884	0.025525	0.282523	-5.03	0.74	0.99	0.03	1.49	0.05	0.282523	-5.16
SY01-20	385	0.282546	0.000022	0.001154	0.032877	0.282537	0.46	0.77	0.97	0.03	1.32	0.05	0.282538	0.17
SY01-23	1110	0.282033	0.000025	0.001036	0.030050	0.282011	-1.51	0.88	1.66	0.03	2.01	0.05	0.282011	-2.35
SY01-26	270	0.282412	0.000015	0.000585	0.015844	0.282409	-6.71	0.53	1.14	0.02	1.67	0.03	0.282409	-6.91
SY01-27	100	0.282461	0.000017	0.002337	0.067802	0.282456	-8.89	0.60	1.12	0.02	1.67	0.04	0.282457	-8.96
SY01-30	99	0.282556	0.000020	0.001180	0.034287	0.282554	-5.47	0.70	0.96	0.03	1.46	0.04	0.282554	-5.55
SY01-31	1734	0.281888	0.000024	0.000912	0.026821	0.281857	7.63	0.84	1.85	0.03	1.93	0.05	0.281858	6.29
SY01-32	2752	0.281174	0.000024	0.001018	0.028525	0.281118	5.61	0.84	2.80	0.03	2.84	0.05	0.281120	3.45
SY01-33	887	0.282068	0.000019	0.000569	0.016267	0.282058	-4.98	0.67	1.59	0.03	2.05	0.04	0.282059	-5.66
SY01-34	239	0.282171	0.000025	0.001679	0.046964	0.282163	-16.11	0.88	1.50	0.03	2.22	0.05	0.282164	-16.28
SY01-35	827	0.281828	0.000055	0.001067	0.022514	0.281811	-15.13	1.93	1.94	0.07	2.62	0.12	0.281811	-15.75
SY01-36	891	0.282075	0.000014	0.000368	0.011211	0.282069	-4.52	0.49	1.58	0.02	2.02	0.03	0.282069	-5.20
SY01-37	178	0.282418	0.000022	0.002315	0.056037	0.282410	-8.76	0.77	1.18	0.03	1.72	0.05	0.282410	-8.89
SY01-38	1266	0.281828	0.000019	0.001102	0.032162	0.281801	-5.32	0.67	1.94	0.03	2.36	0.04	0.281802	-6.28
SY01-39	184	0.282458	0.000013	0.001156	0.035481	0.282454	-7.08	0.46	1.09	0.02	1.63	0.03	0.282454	-7.21
SY01-40	463	0.282366	0.000014	0.001581	0.045321	0.282352	-4.33	0.49	1.23	0.02	1.68	0.03	0.282352	-4.67
SY01-42	648	0.282170	0.000024	0.001204	0.034871	0.282155	-7.06	0.84	1.48	0.03	1.99	0.05	0.282155	-7.54
SY01-43	353	0.282452	0.000014	0.001375	0.042323	0.282443	-3.63	0.49	1.10	0.02	1.55	0.03	0.282443	-3.89
SY01-45	205	0.282634	0.000019	0.005503	0.207105	0.282612	-1.00	0.67	0.96	0.03	1.27	0.04	0.282613	-1.13
SY01-47	454	0.282294	0.000021	0.001285	0.033662	0.282283	-6.98	0.74	1.32	0.03	1.83	0.05	0.282283	-7.31
SY01-48	414	0.282175	0.000019	0.001055	0.030772	0.282167	-12.00	0.67	1.47	0.03	2.11	0.04	0.282167	-12.31
SY01-49	172	0.282324	0.000037	0.000880	0.025801	0.282321	-12.05	1.30	1.26	0.05	1.92	0.08	0.282321	-12.18
SY01-50	1199	0.282172	0.000016	0.001370	0.036668	0.282140	5.15	0.56	1.49	0.02	1.67	0.04	0.282141	4.25
SY01-51	1545	0.282034	0.000022	0.000523	0.015268	0.282018	8.91	0.77	1.64	0.03	1.70	0.05	0.282019	7.71
SY01-54	878	0.282309	0.000017	0.001468	0.040865	0.282284	2.81	0.60	1.30	0.02	1.56	0.04	0.282285	2.16

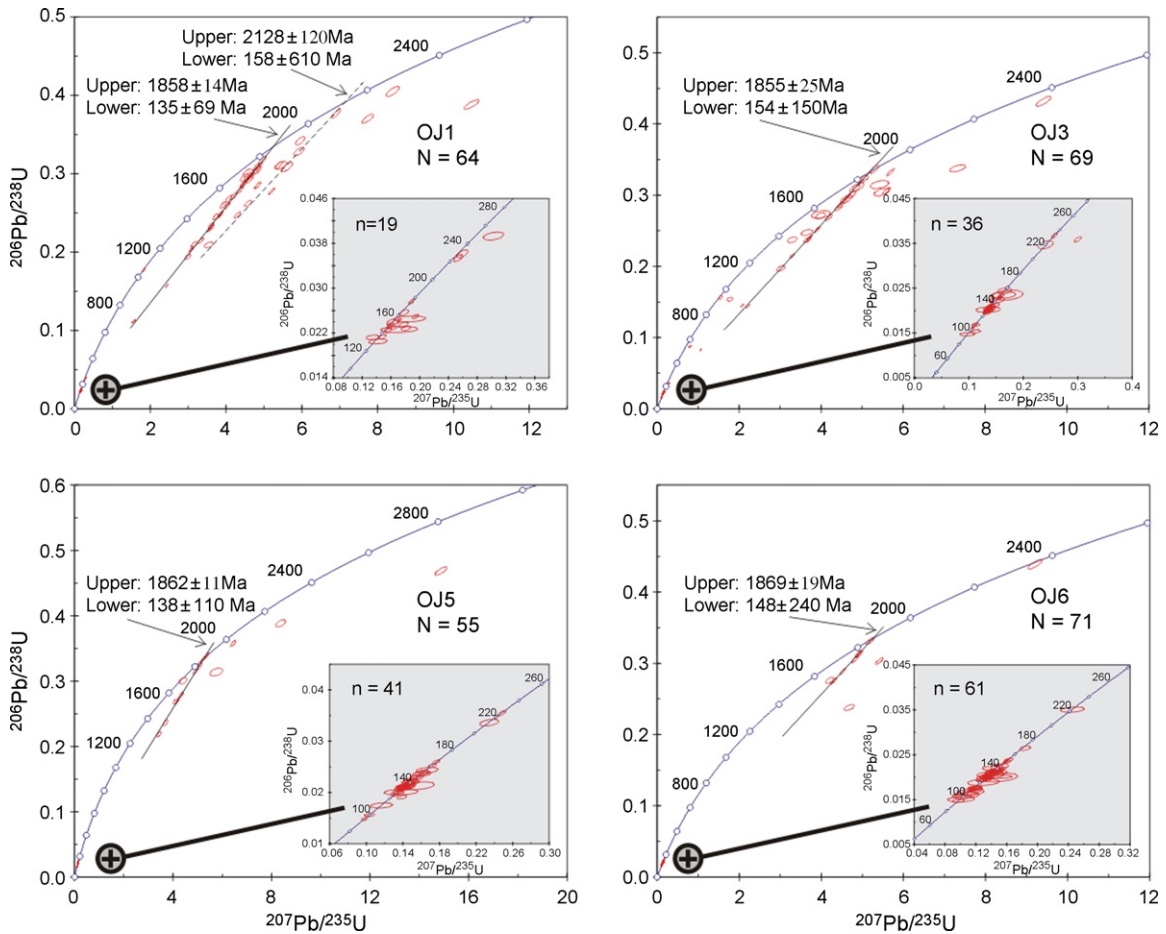


Fig. 2. Concordia plots for eastern Cathaysia (Oujiang River) samples. Insets show expanded plots for younger zircons.

young zircons show good oscillatory zoning, while the older zircons are more homogeneous.

All three samples show a large age range. Most of the zircons are concordant or near-concordant; a few are discordant but no clear discordia trends are apparent (Fig. 4). One near-concordant zircon with a $^{207}\text{Pb}/^{206}\text{Pb}$ age of 3500 Ma (SY01-10, Table 1) is the oldest material yet found in this region.

The age spectrum of these samples is distinctly different from that of the Oujiang River samples (Fig. 5). The Paleoproterozoic ages of 2400–1850 Ma that are prominent in the Oujiang samples are absent, while Neoarchean and Meso-Neoproterozoic ages are common although no prominent peaks are apparent. A Caledonian (ca. 450 Ma) age peak can be clearly recognized, whereas such ages are only weakly represented in the Oujiang samples. The Late Mesozoic ages show a bimodal distribution dominated by Late Jurassic (ca. 160 Ma) grains with a minor Cretaceous (ca. 100 Ma) peak, which is

distinct from the more homogeneous age distribution (130–150 Ma) for the Oujiang region.

4.2. Hf isotopes

Hf-isotope data for 376 zircons are listed in Table 2 and the data are plotted in Fig. 6. More details of the data and implications are described below for Oujiang and North Rivers, respectively.

4.2.1. Oujiang River

All four samples show similar Hf-isotope distribution (Fig. 6). Two Archean zircons plot between the CHUR and Depleted Mantle (DM) lines in Fig. 6, and may reflect the oldest episode of crust growth in eastern Cathaysia. The other scattered zircons from ca. 500 Ma to 1500 Ma lie either above or below the CHUR reference line. These scattered zircons may represent minor magmatic episodes; however, they may also have been

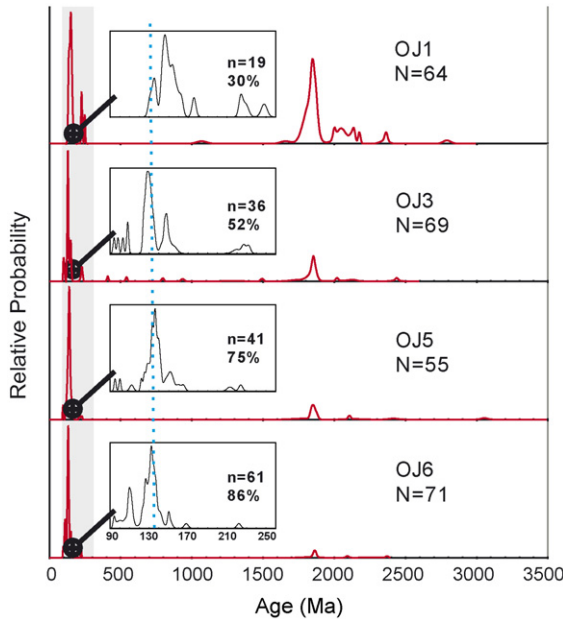


Fig. 3. Age spectra of zircon populations for eastern Cathaysia samples. Insets show Indosian–Yanshanian age range.

affected by non-zero Pb loss due to metamorphic overprinting, in which case the ages are not meaningful.

Paleoproterozoic zircons show three clusters: minor ones at 2400–2300 Ma and 2200–2000 Ma and a major one at ca. 1850 Ma (Fig. 6). The oldest population shows relatively juvenile Hf-isotope compositions. The younger Paleoproterozoic zircons have a large range of ($^{176}\text{Hf}/^{177}\text{Hf}$)_i, plotting either between the CHUR and DM lines or far below the CHUR line in Fig. 6. Model ages (assuming an average-crustal source) for the least radiogenic of these grains extend back to ca. 3.2 Ga, similar to the age of the oldest zircon found in OJ5, while the

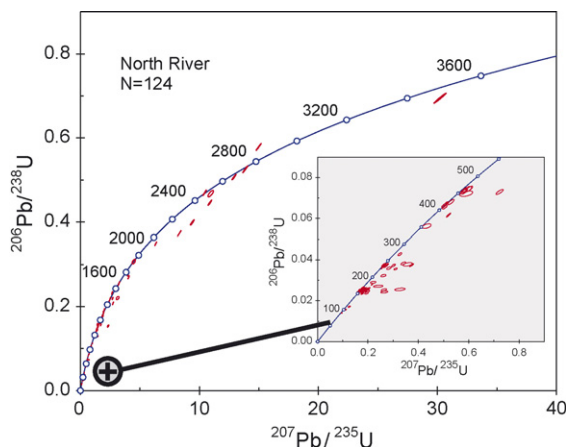


Fig. 4. Concordia plot for western Cathaysia (North River), with expanded area for younger zircons.

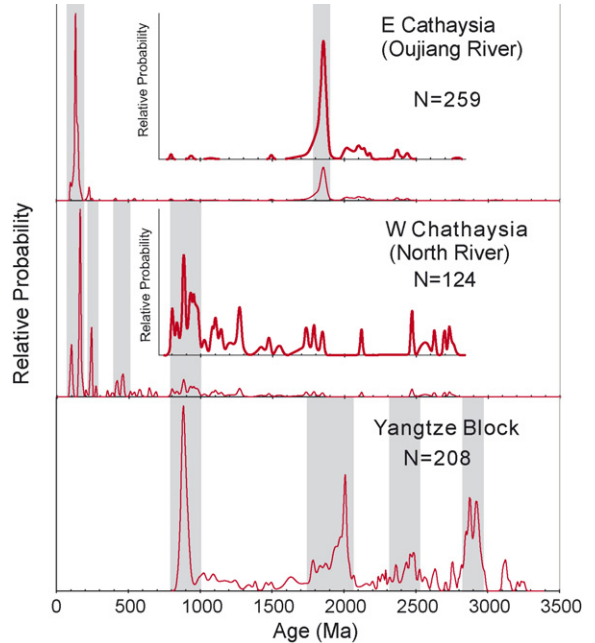


Fig. 5. Age spectra of zircon populations from different areas. Insets show an enlargement for the Precambrian age spectra. Age spectra of Precambrian detrital zircons from the Yangtze Block are shown for comparison; these data are from Gan et al. (1996), X.H. Li et al. (2003), Z.X. Li et al. (2003b), Yin et al. (2003), Jia and Peng (2005), Wu et al. (2006), Zhang et al. (2006a,b), Zheng et al. (2006), Zhou et al. (2006), and Wang et al. (2006).

most radiogenic grains plot near DM. These data suggest that juvenile crustal growth occurred episodically in this region from 2400 Ma to 1850 Ma, and that the younger Paleoproterozoic events also involved extensive reworking of older crust.

The Mesozoic zircons include Indosian (ca. 230 Ma) and Yanshanian ages (ca. 100–150 Ma). The 230 Ma zircons display a large range of ($^{176}\text{Hf}/^{177}\text{Hf}$)_i, but all plot below the CHUR line in Fig. 6. Crustal model ages for the least radiogenic grains extend back to ca. 2.8 Ga, within the range of the oldest zircons found in the same sample. The grain with the most radiogenic Hf gives a crustal model age of 1.85 Ga, corresponding to the main peak of crustal generation observed in these samples. Therefore, zircons with ages of ca. 230 Ma may reflect a thermal event dominated by reworking of Paleoproterozoic to Archean materials in eastern Cathaysia.

The major population of detrital zircons with Yanshanian ages plots below CHUR in Fig. 6, but is generally more radiogenic Hf than the Indosian zircons. Cretaceous zircons have more radiogenic Hf than Jurassic zircons. The crustal model ages for about half of the less radiogenic grains are consistent with derivation from Paleoproterozoic rocks, representing the impor-

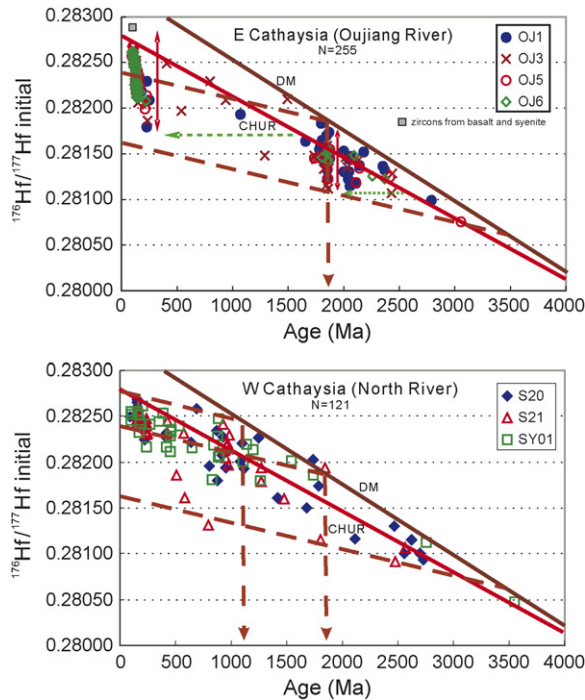


Fig. 6. $(^{176}\text{Hf}/^{177}\text{Hf})_i$ vs. U–Pb age of zircon populations. DM, Depleted Mantle; CHUR, Chondritic Uniform Reservoir. Dashed lines show the evolution of crustal volumes with $^{176}\text{Lu}/^{177}\text{Hf} = 0.015$, corresponding to the average continental crust. The intersection of these lines with the DM curve represents the crustal model age (T_{DM}^{C}) of grains lying along the line.

tant episode of crust growth described above. The more radiogenic grains, with younger model ages, have no corresponding protolith that is represented by older zircons, and suggest mixing between juvenile magmas and those derived from the Paleoproterozoic crust. The Cretaceous juvenile component in Fig. 6 could be represented by zircons (shaded box in Fig. 6) from basalts and syenites that outcrop around the Oujiang catchment region (authors' unpublished data; see below). Therefore, zircons with Cretaceous ages may indicate another episode of juvenile crustal growth in eastern Cathaysia, accompanied by reworking of Paleoproterozoic crustal material.

4.2.2. North River

The oldest zircon (SY01-10) plots between the CHUR and DM lines in Fig. 6. The Neoarchean zircons scatter from the DM line to below CHUR, suggesting an older episode of crustal growth (3.0–3.3 Ga) in western Cathaysia. The Mesoproterozoic zircons show a large range of $(^{176}\text{Hf}/^{177}\text{Hf})_i$. Some grains with lower $(^{176}\text{Hf}/^{177}\text{Hf})_i$ yield Archean model ages, consistent with the protolith defined by the Neoarchean grains in these samples; others suggest juvenile addition.

The Neoproterozoic population also shows a range of $(^{176}\text{Hf}/^{177}\text{Hf})_i$, suggesting a thermal event that involved both juvenile components (points near DM) and reworking of Paleo- to Mesoproterozoic crust (1500–1800 Ma).

Phanerozoic zircons lie below the CHUR reference line, and show a tighter distribution of $(^{176}\text{Hf}/^{177}\text{Hf})_i$ than the Phanerozoic zircons in the samples from eastern Cathaysia. Their crustal model ages are consistent with reworking of the Neoproterozoic crust; since that crust itself represents a mixture of sources, the mean crustal model age of the Phanerozoic zircon populations is ca. 1500 Ma. Thus, the Phanerozoic crustal events in western Cathaysia do not show obvious contributions from juvenile sources, in contrast to their equivalents in eastern Cathaysia.

5. Discussion

5.1. Formation of Paleoproterozoic basement

In the 1990s, Paleoproterozoic high-grade regional metamorphic rocks were recognised in the eastern part of Cathaysia, i.e., the Badu group in SW Zhejiang and the Mayuan group in NW Fujian (Hu et al., 1991a,b; Gan et al., 1993; Zhao et al., 1995; Li et al., 1998; Zhao, 1999). The Badu group consists of felsic gneiss, migmatite and supracrustal rocks. Amphibolites and related metavolcanic rocks from the Badu group yield a Sm–Nd whole-rock isochron age of 2014 ± 43 Ma (Li et al., 1996). Felsic gneisses and migmatites yield zircon U–Pb ages of 1.7–1.9 Ga (Gan et al., 1995), and syn-tectonic granites give similar ages of 1.7–1.9 Ga (Hu et al., 1991a,b; Gan et al., 1995). However, these zircon U–Pb ages are poorly constrained, with numerous discordant zircons but no clearly defined discordia relationships.

The four sand samples from the Oujiang River show relatively well-defined discordia trends; upper (ca. 1850 Ma) and lower (130–150 Ma) intercept ages from the different samples are within error of one another, and suggest Paleoproterozoic magmatism and Jurassic–Cretaceous thermal overprinting. The lower intercept ages are confirmed by the concordant ages of a cluster of zircons in each sample. Another group of zircons defines a discordia trend with an older upper intercept (2128 ± 120 Ma) and a similar (158 ± 610 Ma) lower intercept, but some of these grains may have been affected by reworking events at both 1850 Ma and 130 Ma, and the geological significance of the upper intercept age is not clear. Both U–Pb dating and Hf-isotope analyses of zircons indicate that the oldest crustal growth could extend back to Mesoarchean time, and that

the Paleoproterozoic crust in eastern Cathaysia is partly derived from much older protoliths.

5.2. Late Mesozoic crust–mantle interaction in eastern Cathaysia

The basement of eastern Cathaysia is mostly overlain by a NNE-trending volcanic belt which is dominated by rhyolite, coexisting with minor amounts of andesite and basalt. The volume proportion of basalt is less than 30% even in bimodal volcanic assemblages. The basalts are mainly calc-alkaline rather than tholeiitic. Extensive crust–mantle interaction is reflected in a high degree of crustal contamination of the basalts, and formation of andesitic rocks by mixing between underplating basaltic magma and overlying silicic magmas generated by partial melting of the crust (Xu and Xie, 2005).

The detrital zircons with Late Jurassic to Cretaceous ages (90–140 Ma) show very large ranges of $(^{176}\text{Hf}/^{177}\text{Hf})_i$, suggesting mixing between an old crustal component and a more juvenile one. To further constrain the nature of the juvenile component, we have analysed zircons from one syenite and two basalts from just outside the Oujiang River catchment. These zircons all give $^{206}\text{Pb}/^{238}\text{U}$ ages of ca. 100 Ma; their mean $(^{176}\text{Hf}/^{177}\text{Hf})_i$ lies between CHUR and DM (Fig. 6). The relatively low $(^{176}\text{Hf}/^{177}\text{Hf})_i$ of zircons from these mafic

rocks may reflect either some crustal contamination, or derivation from an enriched mantle source (Griffin et al., 2000). In either case, they provide a minimum value of $(^{176}\text{Hf}/^{177}\text{Hf})_i$ for the mantle contribution to this magmatic event, and this value is slightly higher than the most radiogenic Hf-isotope compositions of the Mesozoic detrital zircons.

The Yanshanian magmatism in this area thus appears to reflect mixing between an old crustal component, probably the Paleoproterozoic basement, and a juvenile one that may be derived from an enriched mantle source. In eastern Cathaysia, the zircons from Yanshanian rocks show a shift with time toward younger T_{DM}^{C} model ages (Table 2 and Fig. 7), suggesting that the proportional contribution of the juvenile mantle increased with time. The U–Pb dating and Hf-isotope analysis of the zircons provide evidence of extensive crust–mantle interaction during Late Mesozoic magmatism.

The four samples from Oujiang show a progressive downstream decrease in the proportion of zircons with Paleoproterozoic and Early Mesozoic ages, whereas the proportion of zircons with Late Jurassic to Cretaceous ages increases. These observations are consistent with available geological mapping. The marked downstream changes in the distribution of age populations emphasize that care needs to be exercised in using detrital zircons to estimate continental growth rates.

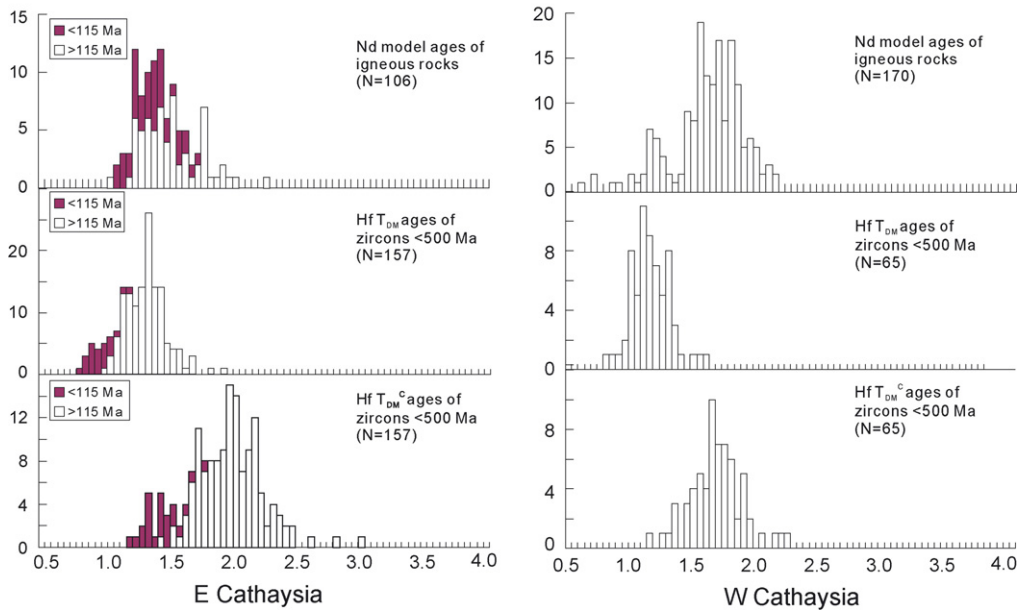


Fig. 7. Distribution of zircon Hf model ages, compared with Nd model ages (T_{DM}) of Mesozoic igneous rocks. Nd model age data are from Shen et al. (2007) and references therein.

5.3. Model ages and crustal genesis

An extensive survey of the Nd-isotope composition of Phanerozoic igneous rocks across Cathaysia (Gilder et al., 1996; Chen and Jahn, 1998; Shen et al., 2007 and references therein) suggests that their basement source rocks were dominantly Proterozoic. Mean $T_{2\text{DM}}$ model ages in western Cathaysia peak around 1.7 Ga, while those in eastern Cathaysia are concentrated around 1.4 Ga (Fig. 7). However, no exposures of Paleoproterozoic basement have been found in western Cathaysia. Previous studies on the volcanic rocks of eastern Cathaysia indicate that those older than 115 Ma show a transition to S-type characteristics, whereas those younger than 115 Ma show I-type signatures (Chen and Jahn, 1998 and references therein). However, most of those older than 115 Ma still have Nd model ages that are younger than the crustal basement ages (1.7–1.9 Ga) (Fig. 7), suggesting the presence of a significant juvenile component.

The zircon data from the present study provide a better understanding of these data, and of the limitations of the model-age approach. In eastern Cathaysia, the ca. 1.4 Ga peak in Nd model ages may not correspond to any real thermal event, but reflects the generation of magmatic rocks by mixing between magmas derived from a juvenile source, and others derived by remelting of a Paleoproterozoic basement (Figs. 6 and 7). In western Cathaysia, the crustal basement rocks are dominantly Neoproterozoic, and the ca. 1.7 Ga peak in Nd model ages corresponds only to a minor population in the zircon age spectrum (Figs. 6 and 7).

These discrepancies simply reflect the complex and extended crustal histories of the two areas; the model-age approach cannot resolve more than one previous event. Thus, the underestimation of the dominant crustal age in eastern Cathaysia arises from the mixing of two sources to produce the Phanerozoic magmatic rocks. The overestimation of the dominant crustal age in western Cathaysia reflects a similar mixing of components during the formation of the Neoproterozoic crust, which in turn served as the source for Phanerozoic magmas.

The same problem would arise from trying to use Hf model ages, which are dominated by the contribution from Hf in zircon (Fig. 7). In eastern Cathaysia, the T_{DM} model ages of the zircons in Phanerozoic magmas are similar to Nd model ages, and do not reflect a real crustal source; “crustal” model ages (T_{DM}^{C} ; Table 2) give a better approximation to the age of the crustal component. However, in western Cathaysia, the opposite is true; T_{DM} model ages of zircons are equivalent to the age of the main crustal source rocks, while T_{DM}^{C} model

ages, like Nd model ages, overestimate the age of this component.

These examples illustrate the power of regional detrital-zircon studies, in which Hf-isotope analysis adds another layer of information to U–Pb age spectra, and makes it possible to unravel the crustal evolution of terrane-scale crustal blocks in more detail.

5.4. Cathaysia: two terranes?

Some previous studies have (implicitly or explicitly) treated Cathaysia as a single tectonic unit, with a Proterozoic basement strongly overprinted by widespread Mesozoic magmatism; Caledonian and Indosinian overprints have been recognised locally in the western part. Geochemical and isotopic data on the Mesozoic igneous rocks have been interpreted in terms of a change from S-type magmatism in the west to I-type in the east.

Our data suggest that the tectonic situation may be more complex. The basement rocks of the two regions studied here, representing drainages of 18,000 km² (Oujiang River, eastern Cathaysia) and 46,000 km² (North River, western Cathaysia), have radically different histories, as illustrated by Figs. 6 and 7. The crust sampled by the Oujiang River was generated in Paleoproterozoic time, with some contribution from Mesoarchean precursors; there is little evidence for thermomagmatic events between 1.8 Ga and Mesozoic time. The crust sampled by the North River contains Neoarchean material, and some evidence for Paleoproterozoic magmatism, but the main episode of crustal generation was in Neoproterozoic time, a period that is not represented in the samples from eastern Cathaysia. The western Cathaysia area experienced strong Caledonian (ca. 450 Ma) and Indosinian (ca. 240 Ma) overprints, which also are not obvious in the Oujiang River catchment. Both eastern and western parts of Cathaysia have age spectra distinct from the Yangtze craton (Fig. 5), which is consistent with previous tectonostratigraphic observations.

These observations suggest to us that the two areas sampled here belong to different terranes, which had quite different evolutionary histories prior to Mesozoic time. The apparent absence of the Caledonian and Indosinian events in the part of eastern Cathaysia sampled here may indicate that the two terranes were not tectonically coupled even during the Indosinian orogeny.

In SE China, large-scale Yanshanian magmatism started from the middle Jurassic, continued for 100 Ma and became most intensive in the Early Cretaceous. Early Yanshanian (180–140 Ma) magmatism is mostly represented by S-type granites in western Cathaysia, but also

involves minor juvenile input as shown by the occurrence of some basalts and gabbros in a narrow EW volcanic belt (Xu and Xie, 2005). Late Yanshanian (140–90 Ma) magmatism is dominated by I-type volcanic-intrusive rocks in eastern Cathaysia (Zhou and Li, 2000).

Our zircon U–Pb age dating and Hf-isotope data are consistent with these earlier observations, which commonly are interpreted in terms of a single tectonic episode with variable effects across the Cathaysia Block (e.g., Chen and Jahn, 1998). However, the marked differences in pre-Yanshanian history between our samples from western and eastern Cathaysia might indicate that these two terranes actually were juxtaposed during the Yanshanian event, possibly along the Zhenghe-Dapu fault, as suggested by Chen and Jahn (1998).

Paleomagnetic data (Gilder et al., 1995, 1996), suggest that western Cathaysia has been linked to the Yangtze Block at least since the Late Permian-Triassic, while Fujian (in the middle of eastern Cathaysia) may have been rotated $121 \pm 9^\circ$ counterclockwise and displaced $22 \pm 9^\circ$ north, relative to western Cathaysia. Gilder et al. (1996) suggested that “the Mesozoic tectonic regime in south China consisted of strike-slip activity . . . as terranes . . . were transported north along sinistral faults”. This model is consistent with our data. Wang et al. (2005) have suggested that the sinistral displacement along the major NE-trending faults may be as old as Permo-Triassic. However, our data would suggest a juxtaposition of eastern and western Cathaysia after the Permian magmatism recognised in western Cathaysia. As shown in Fig. 1, there are several such fault systems within Cathaysia, and these may have different degrees and histories of displacement; the available paleomagnetic data are too few to resolve this question at this stage.

Our data suggest that the internal structure, origin and evolution of Cathaysia, and its role in the assembly of Rodinia, need to be examined more closely. Craton-wide generalities about the origin and evolution of this block, based on available geological and isotopic data, are clearly inadequate. The present study will need to be expanded by more regional and local studies, to test the extent and homogeneity of the distinct patterns of crustal evolution identified here. Such studies may ultimately reveal the presence of several terranes within Cathaysia, and provide new information on the evolution of this major crustal block.

6. Conclusions

Four samples from the Oujiang River in eastern Cathaysia record major crustal growth in Paleo-

proterozoic time and large-scale Jurassic–Cretaceous (Yanshanian) reworking, accompanied by juvenile crustal growth. There is little evidence for thermomagmatic events between 1.8 Ga and the Yanshanian events.

Three samples from the North River reveal that the western Cathaysia crust was generated mainly in Neoproterozoic time, but includes Neoarchean and minor Paleoproterozoic components. This Neoproterozoic crust was reworked in the Caledonian (ca. 450 Ma) and Indosinian (ca. 240 Ma) events, but these are not observed in the Oujiang River samples. The Early Yanshanian magmatism also involved reworking of the older crust, without obvious contributions from juvenile sources. The marked differences in crustal history between the two areas suggest that they represent different terranes, which may be joined along the Zhenghe-Dapu fault. The absence of the Caledonian and Indosinian overprints in the sampled parts of eastern Cathaysia may indicate that the two terranes were separate before Indosinian, or at least Caledonian time, and may only have been juxtaposed by strike-slip movement in Mesozoic time.

Acknowledgments

We are grateful to Suzy Elhlou for her assistance with the analyses. Two anonymous reviewers and editor Cawood provided helpful comments. This work was supported by NSF of China Grants (Nos. 40125007, 40221301), an ARC Discovery Grant (SYO'R and WLG) and an ARC IREX Grant (SYO'R and WLG). This study used instrumentation funded by ARC LIEF and DEST Systemic Infrastructure Grants, Macquarie University and industry. This is publication no. 477 from the ARC National Key Centre for the Geochemical Evolution and Metallogeny of Continents (<http://www.els.mq.edu.au/GEMOC/>).

References

- Ames, L., Zhou, G., Xiong, B., 1996. Geochronology and isotopic character of ultrahigh-pressure metamorphism with implications for collision of the Sino-Korean and Yangtze cratons, central China. *Tectonics* 15, 472–489.
- Barth, A.P., Wooden, J.L., Coleman, D.S., Fanning, C.M., 2000. Geochronology of the Proterozoic basement of southwesternmost North America, and the origin and evolution of the Mojave crustal province. *Tectonics* 19 (4), 616–629.
- Bizzarro, M., Baker, J.A., Haack, H., Ulfbeck, D., Rosing, M., 2003. Early history of Earth's crust–mantle system inferred from hafnium isotopes in chondrites. *Nature* 421, 931–933.
- Blichert-Toft, J., Albarède, F., 1997. The Lu–Hf geochemistry of chondrites and the evolution of the mantle–crust system. *Earth Planet. Sci. Lett.* 148, 243–258.

- Black, L.P., Gulson, B.L., 1978. The age of the Mud Tank carbonatite, Strangways Range, Northern Territory. *BMR J. Aust. Geol. Geophys.* 3, 227–232.
- Cawood, P.A., Nemchin, A.A., Freeman, M., Sircombe, K., 2003. Linking source and sedimentary basin: detrital zircon record of sediment flux along a modern river system and implications for provenance studies. *Earth Planet. Sci. Lett.* 210 (1–2), 259–268.
- Chen, J.F., Jahn, B.-m., 1998. Crustal evolution of southeastern China: Nd and Sr isotopic evidence. *Tectonophysics* 284, 101–133.
- Claesson, S., Bogdanova, S.V., Bibikova, E.V., Gorbatschev, R., 2001. Isotopic evidence for Palaeoproterozoic accretion in the basement of the East European Craton. *Tectonophysics* 339, 1–18.
- Condie, K.C., Beyer, E., Belousova, E., Griffin, W.L., O'Reilly, S.Y., 2005. U–Pb isotopic ages and Hf isotopic composition of single zircons: the search for juvenile Precambrian continental crust. *Precam. Res.* 139 (1–2), 42–100.
- Gan, X., Li, H., Sun, D., 1993. Geochronological study on the Precambrian metamorphic basement in northern Fujian. *Geol. Fujian* 1, 17–32 (in Chinese).
- Gan, X., Li, H., Sun, D., Jin, W., Zhao, F., 1995. A geochronological study on early Proterozoic granitic rocks, southwestern Zhejiang. *Acta Petrol. Mineral.* 14, 1–8 (in Chinese).
- Gan, X., Zhao, F., Jin, W., Sun, D., 1996. The U–Pb ages of early Proterozoic–Archean zircons captured by igneous rocks in southern China. *Geochimica* 25, 112–120 (in Chinese).
- Gao, S., Ling, W., Qiu, Y., Lian, Z., Hartmann, G., Simon, K., 1999. Contrasting geochemical and Sm–Nd isotopic compositions of Archean metasediments from the Kongling high-grade terrain of the Yangtze craton: Evidence for cratonic evolution and redistribution of REE during crustal anatexis. *Geochim. Cosmochim. Acta* 63, 2071–2088.
- Gilder, S.A., Coe, R.S., Wu, H., Kunag, G., Zhao, X., Wu, Q., 1995. Triassic paleomagnetic data from south China and their bearing on the tectonic evolution of the western circum-Pacific region. *Earth Planet. Sci. Lett.* 131 (3–4), 269–287.
- Gilder, S.A., Gill, J., Coe, R.S., Zhao, X.X., Liu, Z.W., Wang, G.X., Yuan, K.R., Liu, W.L., Kuang, G.D., Wu, H.R., 1996. Isotopic and paleomagnetic constraints on the Mesozoic tectonic evolution of south China. *J. Geophy. Res.* 101, 16137–16154.
- Grabau, A.W., 1924. Stratigraphy of China, Part I, Paleozoic and Older Geological Survey of Agriculture and Commerce, Peking, 528 pp.
- Griffin, W.L., Belousova, E.A., Shee, S.R., Pearson, N.J., O'Reilly, S.Y., 2004. Archean crustal evolution in the northern Yilarn Craton: U–Pb and Hf-isotope evidence from detrital zircons. *Precam. Res.* 131, 231–282.
- Griffin, W.L., Belousova, E.A., Walters, S.G., O'Reilly, S.Y., 2006. Archean and Proterozoic crustal evolution in the eastern succession of the Mt Isa District, Australia: U–Pb and Hf-isotope studies of detrital zircons. *Aust. J. Earth Sci.* 53, 125–150.
- Griffin, W.L., Pearson, N.J., Belousova, E.A., Jackson, S.E., O'Reilly, S.Y., van Achterberg, E., Shee, S.R., 2000. The Hf isotope composition of cratonic mantle: LAM-MC-ICPMS analysis of zircon megacrysts in kimberlites. *Geochim. Cosmochim. Acta* 64, 133–147.
- Griffin, W.L., Wang, X., Jackson, S.E., Pearson, N.J., O'Reilly, S.Y., Xu, X.S., Zhou, X.M., 2002. Zircon chemistry and magma genesis, SE China: in-situ analysis of Hf isotopes, Tonglu and Pingtan igneous complexes. *Lithos* 61, 237–269.
- Hong, D.W., Xie, X.L., Zhang, J.S., 1999. An exploration on the composition, nature and evolution of mid-lower crust in south China based on the Sm–Nd isotopic data of granites. *Geol. J. China Univ.* 5, 361–371 (in Chinese).
- Hu, X., Xu, J., Kang, H., Tong, C., Chen, C., Ye, G., 1991a. Geological features of the lower Proterozoic Badu group of southwestern Zhejiang and its implications. *Reg. Geol. China* 3, 234–240 (in Chinese).
- Hu, X., Xu, J., Tong, C., 1991b. The Precambrian Geology of Southwestern Zhejiang Province. Geological Publishing House, Beijing, pp. 1–277 (in Chinese).
- Iizuka, T., Hirata, T., Komiya, T., Rino, S., Katayama, I., Motoki, A., Maruyama, S., 2005. U–Pb and Lu–Hf isotope systematics of zircons from the Mississippi River sand: Implications for reworking and growth of continental crust. *Geology* 33 (6), 485–488.
- Jackson, S.E., Pearson, N.J., Griffin, W.L., Belousova, E.A., 2004. The application of laser ablation-inductively coupled plasma-mass spectrometer (LA-ICP-MS) to *in situ* U–Pb zircon geochronology. *Chem. Geol.* 211, 47–69.
- Jahn, B.M., Zhou, X.H., Li, J.L., 1990. Formation and tectonic evolution of Southeastern China and Taiwan: isotopic and geochemical constraints. *Tectonophysics* 183, 145–160.
- Jia, B.H., Peng, H.Q., 2005. Precambrian Geology and Mineralization in Northeast Hunan. Geological Publishing House, Beijing, pp. 72–75 (in Chinese).
- Lan, C.-Y., Chung, S.-L., Lo, C.-H., Lee, T.-Y., Wang, P.-L., Li, H., Toan, D.V., 2001. First evidence for Archean continental crust in northern Vietnam and its implications for crustal and tectonic evolution in Southeast Asia. *Geology* 29, 219–222.
- Lan, C.-Y., Chung, S.-L., Long, T.V., Lo, C.-H., Lee, T.-Y., Mertzman, S.A., Shen, J.J.-S., 2003. Geochemical and Sr–Nd isotopic constraints from the Kontum massif, central Vietnam on the crustal evolution of the Indochina block. *Precam. Res.* 122, 7–27.
- Li, S., Chen, Y., Ge, N., Hu, X., Liu, D., 1996. Isotopic ages of metavolcanic rocks and metacrust mylonite in the Badu group in southwestern Zhejiang province and their implications for tectonics. *Acta Petrol. Sinica* 12, 79–87 (in Chinese).
- Li, X.H., Li, Z.X., Ge, W.C., Zhou, H.W., Li, W.X., Liu, Y., Wingate, M.T.D., 2003. Neoproterozoic granitoids in South China: crustal melting above a mantle plume at ca. 825 Ma? *Precam. Res.* 122, 45–83.
- Li, X.H., Sun, M., Wei, G.J., Liu, Y., Lee, C.Y., Malpas, J., 2000. Geochemical and Sm–Nd isotopic study of amphibolites in the Cathaysia Block, southeastern China: evidence for an extremely depleted mantle in the Paleoproterozoic. *Precam. Res.* 102, 251–262.
- Li, X.H., Wang, Y., Zhao, Z., Chen, D., 1998. SHRIMP U–Pb zircon geochronology for amphibolite from the Precambrian basement in SW Zhejiang and NW Fujian provinces. *Geochimica* 27, 327–334 (in Chinese).
- Li, Z.X., 1998. Tectonic history of the major east Asian lithospheric blocks since the mid-Proterozoic—a synthesis. In: Flower, M.F.J., Chung, S.L., Lo, C.H., Lee, T.Y. (Eds.), *Mantle Dynamics and Plate Interactions in East Asia, Geodynamics Series*, vol. 27. American Geophysical Union, Washington, DC, pp. 221–243.
- Li, Z.X., Cho, M., Li, X.-H., 2003a. Precambrian tectonics of East Asia and relevance to supercontinent evolution. *Precam. Res.* 122, 1–6.
- Li, Z.X., Li, X.H., Kinny, P.D., Wang, J., Zhang, S., Zhou, H.W., 2003b. Geochronology of Neoproterozoic syn-rift magmatism in the Yangtze Craton, South China and correlations with other continents: evidence for a mantle superplume that broke up Rodinia. *Precam. Res.* 122, 85–109.
- Li, Z.X., Li, X.H., Zhou, H.W., Kinny, P.D., 2002. Grenvillian continental collision in south China: New SHRIMP U–Pb zircon results and implications for the configuration of Rodinia. *Geology* 30, 163–166.

- Ludwig, K.R., 2000. Isoplot/Ex version 2.3.—a geochronological toolkit for Microsoft Excel. Berkeley Geochronology Center. Special Publication No. 1a. Berkeley.
- Neves, S.P., 2003. Proterozoic history of the Borborema province (NE Brazil): Correlations with neighboring cratons and Pan-African belts and implications for the evolution of western Gondwana. *Tectonics* 22 (4), Art. No. 1031.
- Qiu, Y., Gao, S., McNaughton, N.J., Groves, D.I., Ling, W., 2000. First evidence of >3.2 Ga continental crust in the Yangtze craton of south China and its implications for Archean crustal evolution and Phanerozoic tectonics. *Geology* 28, 11–14.
- Rino, S., Komiya, T., Windley, B.F., Katayama, I., Motoki, A., Hirata, T., 2004. Major episodic increases of continental crustal growth determined from zircon ages of river sands; implications for mantle overturns in the Early Precambrian. *Phys. Earth Planet. Inter.* 146 (1–2), 369–394.
- Scherer, E., Munker, C., Mezger, K., 2001. Calibration of the lutetium–hafnium clock. *Science* 293, 683–687.
- Shen, W.Z., Ling, H.F., Sun, T., 2007. Sr, Nd isotope geochemistry of Late Mesozoic granite and volcanic rocks in South China. In: *Genesis of Late Mesozoic Granites and Lithospheric Dynamics in Nanling Region*. Science Press, Beijing (Chapter 6).
- Shui, T., 1987. Tectonic framework of the southeastern China continental basement. *Sci. China B* 30, 414–422 (in Chinese).
- Wang, Q., Li, J.W., Jian, P., Zhao, Z.H., Xiong, X.L., Bao, Z.W., Xu, J.F., Li, C.F., Ma, J.L., 2005. Alkaline syenites in eastern Cathaysia (South China): link to Permian–Triassic transtension. *Earth Planet. Sci. Lett.* 230, 339–354.
- Wang, X.L., Zhou, J.C., Qiu, J.S., Zhang, W.L., Liu, X.M., Zhang, G.L., 2006. LA-ICPMS U–Pb zircon geochronology of the Neoproterozoic igneous rocks from Northern Guangxi, South China: implications for petrogenesis and tectonic evolution. *Precam. Res.* 145, 111–130.
- Wiedenbeck, M., Allé, P., Corfu, F., Griffin, W.L., Meier, M., Oberli, F., von Quadt, A., Roddick, J.C., Spiegel, W., 1995. Three natural zircon standards for U–Th–Pb, Lu–Hf, trace element and REE analyses. *Geostand. Newslett.* 19, 1–23.
- Wu, R.X., Zheng, Y.F., Wu, Y.B., Zhao, Z.F., Zhang, S.B., Liu, X.M., Wu, F.Y., 2006. Reworking of juvenile crust: element and isotopic evidence from Neoproterozoic granodiorite in South China. *Precam. Res.* 146, 179–212.
- Xu, X.S., Xie, X., 2005. Late Mesozoic–Cenozoic basaltic rocks and crust–mantle interaction, SE China. *Geol. J. China Univ.* 11 (3), 318–334 (in Chinese).
- Yin, C.Y., Liu, D.Y., Gao, L.Z., Wang, Z.Q., Xing, Y.S., Jian, P., Shi, Y.R., 2003. Lower boundary age of the Nanhua System and the Gucheng glacial stage: evidence from SHRIMP II dating. *Chin. Sci. Bull.* 48 (16), 1657–1662.
- Zhang, S.B., Zheng, Y.F., Wu, Y.B., Zhao, Z.F., Gao, S., Wu, F.Y., 2006a. Zircon isotope evidence for ≥3.5 Ga continental crust in the Yangtze craton of China. *Precam. Res.* 146, 16–34.
- Zhang, S.B., Zheng, Y.F., Wu, Y.B., Zhao, Z.F., Gao, S., Wu, F.Y., 2006b. Zircon U–Pb age and Hf–O isotope evidence for Paleoproterozoic metamorphic event in South China. *Precam. Res.* 151, 265–288.
- Zhao, G., Peter, A.C., 1999. Tectonothermal evolution of the Mayuan assemblage in the Cathaysia block: implications for Neoproterozoic collision-related assembly of the South China craton. *Am. J. Sci.* 299, 309–339.
- Zhao, F., 1999. The chronotectonic framework of Pre-Caledonian basements from Cathaysia block. *Prog. Precam. Res.* 22, 39–46 (in Chinese).
- Zhao, F., Jin, W., Gan, X., Sun, D., Wang, Z., 1995. Discussions on the characteristics of the deep crust and Pre-Caledonian metamorphic basement in the Cathaysia block, southeastern China. *Acta Geosci. Sinica* 3, 235–245 (in Chinese).
- Zheng, J.P., Griffin, W.L., O'Reilly, S.Y., Zhang, M., Pearson, N.J., Pan, Y.M., 2006. Widespread Archean basement beneath the Yangtze craton. *Geology* 34 (6), 417–420.
- Zhou, M.F., Ma, Y.X., Yan, D.P., Xia, X.P., Zhao, J.H., Sun, M., 2006. The Yanbian Terrane (Southern Sichuan Province, SW China): a Neoproterozoic arc assemblage in the western margin of the Yangtze Block. *Precam. Res.* 144, 19–38.
- Zhou, X.M., Li, W.X., 2000. Origin of Late Mesozoic igneous rocks of Southeastern China: implications for lithosphere subduction and underplating of mafic magmas. *Tectonophysics* 326, 269–287.